TU Delft

Delft University of Technology

A mathematical programming model for optimal fleet management of electric car-sharing systems with Vehicle-to-Grid operations

Prencipe, Luigi Pio; Theresia van Essen, J.; Caggiani, Leonardo; Ottomanelli, Michele; Homem de Almeida Correia, Gonçalo

DOI
10.1016/j.jclepro.2022.133147

Publication date
2022

Document Version
Final published version

Published in
Journal of Cleaner Production

Citation (APA)
Prencipe, L. P., Theresia van Essen, J., Caggiani, L., Ottomanelli, M., & Homem de Almeida Correia, G. (2022). A mathematical programming model for optimal fleet management of electric car-sharing systems with Vehicle-to-Grid operations. *Journal of Cleaner Production*, *368*, Article 133147. https://doi.org/10.1016/j.jclepro.2022.133147

Important note
To cite this publication, please use the final published version (if applicable).
Please check the document version above.

Copyright
Other than for strictly personal use, it is not permitted to download, forward or distribute the text or part of it, without the consent of the author(s) and/or copyright holder(s), unless the work is under an open content license such as Creative Commons.

Takedown policy
Please contact us and provide details if you believe this document breaches copyrights.
We will remove access to the work immediately and investigate your claim.

This work is downloaded from Delft University of Technology.
For technical reasons the number of authors shown on this cover page is limited to a maximum of 10.

Green Open Access added to TU Delft Institutional Repository

'You share, we take care!' - Taverne project

https://www.openaccess.nl/en/you-share-we-take-care

Otherwise as indicated in the copyright section: the publisher is the copyright holder of this work and the author uses the Dutch legislation to make this work public.

Journal of Cleaner Production 368 (2022) 133147

Contents lists available at ScienceDirect

Journal of Cleaner Production

journal homepage: www.elsevier.com/locate/jclepro

A mathematical programming model for optimal fleet management of electric car-sharing systems with Vehicle-to-Grid operations

Luigi Pio Prencipe [a,*], J. Theresia van Essen [b], Leonardo Caggiani [a], Michele Ottomanelli [a], Gonçalo Homem de Almeida Correia [c]

[a] Department of Civil, Environmental, Building and Land Engineering and Chemistry, Polytechnic University of Bari, Bari, Italy
[b] Delft Institute of Applied Mathematics, Delft University of Technology, Delft, the Netherlands
[c] Department of Transport & Planning, Delft University of Technology, Delft, the Netherlands

ARTICLE INFO

Handling Editor: Zhifu Mi

Keywords:
V2G
One-way electric car-sharing
Electric vehicles
Mixed integer linear programming
Shared mobility

ABSTRACT

Electric car-sharing systems have attracted large attention in recent years as a new business model for achieving both economic and environmental benefits in urban areas. Among different types, the one considered in this paper is the so-called one-way car-sharing system whereby a user can begin and end a trip at any station of the system. At the same time, the Vehicle-to-Grid (V2G) concept is emerging as a possible innovative solution for smart power grid control. A management system that combines car-sharing system operations and V2G technology is a recent challenge for academia and industry. In this work, a mixed integer linear programming formulation is proposed to find the optimal management of electric vehicles in a one-way car-sharing system integrated with V2G technology. The proposed mathematical model allows finding the optimal start-of-day electric vehicles distribution that maximizes the total revenue obtained from system users and V2G profits through daily electric vehicles charging/discharging schedules. These schedules are based on mean daily users' electric vehicles requests and electricity prices. The model can be applied to evaluate the possible average daily profitability of V2G operations. In order to test the model performance, we applied it to a small-size test network and a real-size test network (the Delft network in the Netherlands). Under the model assumptions, the adoption of V2G technology allows to fully cover the daily charging costs due to users' trips and to obtain V2G profits by taking advantage of electric vehicles unused time without significantly reducing the satisfied car-sharing system demand. Most of the energy purchased to charge the electric vehicles batteries is provided back to the grid during energy peak load demand, creating benefits also for energy providers.

1. Introduction

Shared mobility is one of the possible solutions for reducing the traffic congestion problem. It offers the potential to enhance the efficiency, competitiveness, social equity, and quality of life in large cities (Machado et al., 2018). Among the different shared mobility modes, such as bike-sharing, car-pooling, and peer-to-peer ridesharing, car-sharing is the most known and widespread system used in urban areas. In the literature, one can find plenty of literature regarding Car-Sharing Systems (CSSs) demand and supply in the last years. Generally, CSSs are classified as station-based (one-way or two-way), free-floating, or hybrid systems. Station-based CSSs allow users to pick-up and drop-off a car only in stations. In one-way station-based CSSs, the available cars are distributed in predefined parking places and the departure station can differ from the arrival one (Nourinejad and Roorda, 2015; Boyacı et al., 2015; Correia et al., 2014). In two-way station-based CSSs, the predefined parking places remain, but users have to return cars to the pick-up stations (Nourinejad and Roorda, 2015). Free-floating systems are the most recent ones. They offer the possibility to park a rented car in any public space of the operational area served by car-sharing companies (Firnkorn and Müller, 2011; Li et al., 2018). Finally, CSSs hybrid systems are a combination of both two-way and one-way CSSs station-based types (Jorge et al., 2015a,b) or a combination of a station-based and a free-floating system (Ciari et al., 2014).

In the beginning, CSSs were based on internal combustion engine vehicles. However, CSSs with Electric Vehicles (EVs) have also recently emerged as a need to reduce local pollutants in cities. Indeed, electric

* Corresponding author.
E-mail address: luigipio.prencipe@poliba.it (L.P. Prencipe).

https://doi.org/10.1016/j.jclepro.2022.133147
Received 27 September 2021; Received in revised form 20 June 2022; Accepted 12 July 2022
Available online 18 July 2022
0959-6526/© 2022 Elsevier Ltd. All rights reserved.

mobility has been overgrowing in recent years. In 2019, the global electric car fleet reached around 7.2 million units, recording a yearly 40% increase (IEA, 2020). Following the same trend, the number of EVs worldwide overcomes 10 million units in 2020 (IEA, 2021). The concept of shared mobility with EVs is currently one of the main topics in transportation research and practice as it has the potential to contribute to sustainability in urban areas (Axsen and Sovacool, 2019). If combined with EVs, shared mobility could give another significant contribution to reducing pollution, in terms of Greenhouse Gases (GHGs) and local pollutants as defended by several papers (Requia et al., 2018; Martin and Shaheen, 2011; Jung and Koo, 2018).

Considering the EVs increasing and overall adoption, a future problem could be the large-scale energy supply system (Kongjeen and Bhumkittipich, 2018) of EVs. A large number of EVs could cause several power system issues, including voltage regulation, peak-load demand, frequency variations, and harmonic contamination. A smart grid system can manage the EVs integration and fleet planning to reduce power system stress to a minimum (Ul-Haq et al., 2016). According to the Global EV Outlook 2020 of the International Energy Agency (IEA, 2020), a smart EV charging system can improve power systems through the supply of Demand-Side Response (DSR) services by optimizing the electricity demand pattern. In particular, EVs have the potential to provide energy back to the grid when the energy is needed, i.e., during power demand peak-loads, and to use excess energy from the grid for recharging the EVs battery. The idea is to use EVs battery as a source of energy storage, considering the fast and precise control signals to provide DSR services and to participate in electricity markets. The technology whereby EVs supply power to the network is called Vehicle-to-Grid (V2G). V2G technology aims to involve EV owners in a new 'energy sharing' concept by providing economic benefits. Applied on a large-scale scenario, V2G technology can have multiple advantages in terms of emissions reduction (Saber and Venayagamoorthy, 2010), electric supply network support (Kempton and Letendre, 1997; Kempton and Tomic, 2005b; Guille and Gross, 2009), and economic revenues for EVs owners (Taiebat and Xu, 2019).

To the best of our knowledge, in the literature, only a few authors have analyzed V2G integration in CSSs (Freund et al., 2012; Fournier et al., 2014; Khalen et al., 2018; Iacobucci et al., 2019; Mamalis et al., 2019; Shuyun et al., 2019; Caggiani et al., 2020; Zhang et al., 2020; Li et al., 2022). This paper aims to propose and test, for a one-way CSS with EVs, a novel Mixed Integer Linear Programming (MILP) model. This formulation determines EVs distribution among stations at the beginning of the day and finds the optimal daily EVs charging/discharging schedules. In particular, the objective is to maximize the sum of revenues from system users (CSS revenues) and V2G profits. CSS revenues and V2G profits are obtained according to mean expected daily customer demand and energy sale/purchase criterion based on mean expected day-ahead market electric energy price variation. This model can be applied to evaluate the possible average daily profitability of V2G operations where the fleet and CSS size is fixed. A numerical application on a synthetic case-study and a real network with sensitivity analysis has been performed to show the proposed model effectiveness.

The paper is organized as follows: Section 2 presents the literature review related to CSSs and V2G technology, highlighting the contribution of this paper. Section 3 describes the proposed mathematical formulation considering two approximations of EV charging/discharging function. Section 4 focuses on the model application and presents a small-size case and a real-case network of the city of Delft, the Netherlands including a sensitivity analysis. Section 5 shows the main conclusions and future research that can be developed based on the current work.

2. Literature review

One of the outputs of the proposed model is the start-of-day EVs distribution. Different indicators related to vehicle distribution among stations have been defined to evaluate the performances of a CSS. In Section 2.1, we summarize these indicators proposed in the literature. However, they are not sufficient for optimized fleet management in a V2G framework. Therefore, in Sections 2.2 and 2.3, we present the characteristics/advantages of V2G technology and the literature studies on electric CSSs with V2G charging stations, respectively, to show the motivations and objectives of our research.

2.1. Car-sharing vehicle distribution key performance indicators

One of the main problems related to vehicle distribution among stations in a one-way CSS is vehicle relocation. One-way CSS is the most attractive one since it allows users to make one-way trips. However, one-way operations, as well as the imbalance of vehicle demand, could generate some problems both at the origin (pick-up station) and at the destination (drop-off station) of a trip. Among the possible issues, there is the situation in which vehicles are accumulated in stations where they are not needed, while at the same time, there could be vehicle shortage at stations where more vehicles are required (Barth et al., 2004; Di Febbraro et al., 2012). Due to this imbalance among stations, some users could leave the system because they may not find a car/parking place available near their origin/destination. For this reason, it is necessary to relocate vehicles rebalancing their distribution.

Vehicle relocation, i.e., transfer of vehicles from stations with high vehicle accumulation to stations with low vehicle stock, is a technique that has been proposed to reduce the imbalance of one-way CSSs (Jorge et al., 2014). Thus, the relocation activities allow for rebalancing the CSS to satisfy as many customers as possible. Two main relocation approaches have been proposed in the literature: user-based and operator-based. User-based strategies offer customers incentives for changing their travel behavior. In contrast, operator-based procedures entail vehicle redistributions performed by operators: during the night, when the demand is negligible (static relocation), or during the whole day when the demand changes depending on time (dynamic relocation). Both static and dynamic operator-based car-sharing relocation strategies require personnel costs. However, the relocation costs may be covered and eventually overcome by higher revenues due to the higher percentage of user demand satisfaction. According to Jorge et al. (2014), real-time relocation operations combined with optimization techniques may significantly increase CSS profits. More recently, Santos and Correia (2019) proposed a carpooling of staff operator strategy for the one-way station-based CSS relocation with extra-cost reduction. Additionally, they state that the high costs of relocations would have more effect on CSSs operator profits only through future vehicle automation.

In the literature, several one-way car-sharing relocation models have been proposed. A recent and exhaustive literature review has been written by Illgen and Höck (2019), which the reader can further check. To define the optimal distribution of vehicles among different locations, these models define several Key Performance Indicators (KPIs). Among the first indicators proposed are those related to time, i.e., 'zero-vehicle-time' and 'full-port-time'. The 'zero-vehicle-time' (Barth and Todd, 1999; Kek and Cheu, 2006; Kek et al., 2009) occurs when a station has no parked vehicles. The full-port-time (Kek and Cheu, 2006; Kek et al., 2009), where 'port' means a parking place, occurs when a station is full of parked vehicles reserved by other users. Both 'zero-vehicle-time' and 'full-port-time' reduce the attractiveness of a CSS and can imply a loss of revenues for CSS operators.

Other KPIs presented in the literature are the 'vehicle-to-trip ratio', the 'number of relocations', and the 'number of trips' indicators. The 'vehicle-to-trip ratio' (Barth and Todd, 1999) or 'vehicle-to-trip station ratio' (Kek et al., 2009) evaluates the CSS performance by adding/-removing vehicles or stations in the system. The 'number of relocations' evaluates the CSS performance by applying different relocation policies or strategies (Barth et al., 2004; Jorge et al., 2014; Kek et al., 2009; Nourinejad and Roorda, 2015). Finally, the 'number of trips' indicator provides necessary information about the percentage of satisfied

demand (Jorge et al., 2014; Nair and Miller-Hooks, 2014) by counting all completed trips made by customers. Additionally, the 'number of trips' indicator can be used to evaluate the level of service offered to the clients (Alfian et al., 2014; Fink and Reiners, 2006; Nair and Miller-Hooks, 2010) or the actual vehicle utilization (Alfian et al., 2014). Recently, Prinz et al. (2021) suggested that using KPIs in CSS would improve their service quality, profit, and relocation performance.

In the model proposed in this paper, one of the KPIs used in the objective function is related to the 'number of trips'. It is defined as 'CSS revenues KPI', namely the total revenue obtained from the CSS users paid fee. However, to take advantage of V2G technology, this KPI is not enough for evaluating the proper start-of-day distribution of vehicles to be achieved through a static relocation (operator-based), as explained in the next sub-sections.

2.2. Vehicle-to-Grid concept

According to demand-response services, the V2G concept was first proposed by Kempton and Letendre (1997) and consists of enabling EVs to share the energy from and to the power grid bidirectionally. The batteries of electric vehicles act as a form of distributed energy storage and can transfer electricity from EVs to the power grid and vice versa. Therefore, V2G allows to charge EV batteries during low demand times and to send electricity back to the grid during periods of high demand (Kempton and Tomic, 2005a; 2005b). Before introducing V2G technology, the electric energy transfer between the power grid and EV batteries was only unidirectional, named grid-to-vehicle (G2V). The bidirectional energy flow was successfully implemented by providing energy and ancillary services to the electric grid from EVs. Smart charging systems and aggregators are required for EVs participating in V2G, where multiple EVs can be considered a single unit (Han et al., 2010; Kempton and Tomic, 2005b).

To demonstrate V2G benefits, several authors have analyzed the interconnection between EVs energy storage and the power grid (Kempton and Kubo, 2000; Kempton and Tomic, 2005a, 2005b; Kempton et al., 2005; Williams and Kurani, 2006; Tomic and Kempton, 2007). According to Kaur et al. (2019) and Liu et al. (2019), V2G technology has the potential to transform EVs into a distributed energy resource with multiple benefits for smart grid integration. According to Noel et al. (2019), V2G technology implemented on EVs can provide several advantages in technical, economic, and environmental benefits. Technical benefits are related to the power grid operator. They include voltage regulation (Rogers et al., 2010), spinning reserve (Pavic et al., 2015), load peak shifting (Dallinger et al., 2011), and frequency regulation (Kolawole and Al-Anbagi, 2019). Among the environmental benefits, V2G technology can incentivize the electricity sector decarbonization if combined with renewable power sources (i.e., solar photovoltaic and wind energy) in terms of higher flexibility and backup storage (Noel et al., 2019; Saber and Venayagamoorthy, 2010). Finally, the economic benefits obtained by V2G technology can be classified according to the different stakeholders: EV owners, grid operators, and society. EV owners can get a new revenue source by selling/purchasing electric energy stored in EV batteries to the distributed system operator for different prices during the day. For grid operators and society, V2G can provide cheaper electricity market alternatives. However, quantifying V2G economic benefits is still fuzzy due to different objectives, market, and technical conditions (Heilmann and Friedl, 2021). A smart charging system may manage profits obtained from the purchase and sale of electric energy to identify the most favorable time intervals with the most profitable tariffs during the day to maximize profits. This management is possible given that energy demand response from the power grid is higher during the daytime (daily peaks) and, consequently, the energy tariff is higher. In contrast, the energy demand response from the power grid is lower during the night (off-peak hours, overnight), thus the energy tariff is lower. This process could allow small profits per vehicle per day, however, considering a large-scale EV fleet, the aggregation of all EVs energy transfer may be relevant in terms of profit per kWh. As an example of a future real application, V2G technology can be used to support the energy demand response of a corporate office building by using EVs during an idle time, particularly for air conditioning energy load during the summer period. Recently, Li et al. (2021b) proposed a hierarchical scheduling method of the active distribution network considering flexible loads, i.e., the heating, ventilation, air-conditioning, and EV charging systems, in office buildings calculating the optimal EV daily charging time.

Yilmaz and Krein (2013) and Arfeen et al. (2019) have analyzed the differences between uncoordinated and coordinated smart charging/-discharging systems, highlighting strengths and weaknesses of both methodologies in terms of requirements, costs, and impact on power distribution networks. The uncoordinated charging system allows the EVs charging at any time when plugged into charging columns. In contrast, the coordinated charging/discharging system allows the bidirectional energy transfer between EV batteries and the power grid in a specific time interval managed by a smart strategy. Several authors have addressed the smart charging/discharging system in the literature, focusing on power daily load curve (Zhang et al., 2012; Lassila et al., 2012), economic benefits for EV owners (Fan, 2012), operation costs (Rotering and Ilic, 2011) and power losses (Dallinger et al., 2011). Recently, Cai et al. (2018) have proposed a day-ahead optimal charging/discharging scheduling for EVs considering random initial EV batteries State of Charge (SOC).

In recent years, V2G implementation is a challenge. The diffusion of V2G is still in the first-step stage of development limited to fleet-based pilot projects worldwide (Sovacool et al., 2018). However, several pilot programs are presenting encouraging results by using the bidirectional flow of electricity between EVs and the power grid. Companies involved in the processes of generation, transmission, distribution, and consumption of energy can take advantage of this new functionality given that V2G may prove to be effective in balancing the grid while yielding economic benefits (Modumudi, 2019). Recently, several pilot projects concerning V2G technology implementation are in progress, e.g., Enel and Nissan projects (Enel, 2020), Smart Solar Charging (De Brey, 2017), WeDriveSolar project (WeDriveSolar, 2020), Engie eps and FCA project 2020 (Engie-FCA project, 2020), and different countries Nuvve projects (Nuvve, 2020). For a summary of recent worldwide V2G pilot applications, see Ravi and Aziz (2022). V2G technology adoption may depend on further aspects, such as the fleet market trend, users' preferences, infrastructures, and policies. Meelen et al. (2021) evaluated the level of impact on the upscaling potential of V2G by analyzing socio-technical trends through a system-level account approach. According to Noel et al. (2021), V2G adoption should be encouraged by user-based innovations by evaluating three concepts, i.e., tinkering, testing, and tacit knowledge. Following these concepts, the proposed work can provide a testing contribution from car-sharing and grid operators' perspectives, to evaluate economic and energy potential benefits applied to a specific real network.

2.3. V2G smart charging and car-sharing systems: contribution and outline

The first steps to develop EV charging algorithms in a one-way station-based electric CSSs have been published by Gambella et al. (2018), Brendel et al. (2018), and Illgen and Höck (2018). However, these models do not consider selling energy to the power grid but only G2V optimization, that is, from the power grid to the vehicle perspective.

In the literature, the first models applied to V2G and CSSs were introduced by Freund et al. (2012) and Fournier et al. (2014). Freund et al. (2012) presented a software agent control architecture considering distribution system operators, micro smart grid operators, and car-sharing operators to maximize the EVs charging through the utilization of renewable energy sources. Fournier et al. (2014) analyzed the integration of electric car-sharing fleets implemented with V2G

technology. They estimated the potential profit through the use of a Monte Carlo simulation model with real car-sharing data.

Khalen et al. (2018) developed a mixed rental-trading strategy that predicts the day-ahead electricity prices and demand for each city district, including uncertainties. The authors provided the optimal EV SOC management for maximizing V2G profit for fleet owners and validate the proposed strategy using real-life data of a CSS. Iacobucci et al. (2019) proposed two model-predictive control optimization algorithms for shared autonomous electric vehicles. They optimize V2G charging, routing, and relocation simultaneously. Mamalis et al. (2019) developed a queuing-theoretic model and several computational tools for coordinating EVs in car-sharing service platforms. The authors have assumed that an EV battery can be divided into two distinct parts: the car-sharing service and the grid service part. The model provides an algorithm to optimize the transportation price and the EV battery split percentage for dual-use. Shuyun et al. (2019) introduced a dynamic pricing scheme for the EV-sharing network. The authors formulated the dynamic pricing scheme as an optimization problem that maximizes the system profit considering EVs relocation and Vehicle-Grid integration. Caggiani et al. (2020) proposed to optimize the start-of-day distribution of EVs between CSS depot and the service area and among stations. The two suggested models maximize the difference between V2G profits (coming from the EVs in the depot and the service area) and the lost revenue due to lost users (unsatisfied demand). These models have been solved with a heuristic and using a CSS simulator. Zhang et al. (2020) introduced a two-stage mathematical formulation that evaluates CSS design and EVs profitability by integrating V2G technology. They applied a linear-decision-rule-based approximation approach for solving dynamic operations, considering the minimization of overall costs as the primary objective function. Finally, recent work has been done by Li et al. (2022) related to EV sharing optimization with V2G operations considering electricity price stochasticity. The authors formulated the problem as a Markov decision problem which is solved with a dynamic programming algorithm. The problem is generalized for EV fleet location for obtaining optimal V2G profits according to the electricity market but it does not properly match reservation-based one-way CSSs functioning and EV fleet relocation between stations by including CSS revenues in the objective function.

From the literature arises the need to consider the maximization of possible V2G profits in fleet management. However, this should not reduce revenues from system users. Indeed, if the power grid uses an EV, it lowers its SOC and could be unavailable to users if the SOC falls below a certain threshold level. On the other hand, if an EV is expected to remain unused, it could be worthwhile to sell the energy stored in its battery if the power selling price is higher than the power purchase price. For this reason, in this paper, we propose a model that, starting from a fixed fleet size, aims to find the optimal start-of-day EVs distribution among stations and the optimal energy sale/purchase scheduling for each EV. These two outputs of the problem are defined by maximizing the sum of revenues from CSS users and V2G profits. Therefore, in addition to the 'CSS revenues KPI', we introduce the 'V2G profits KPI' resulting from smart charging and depending on mean expected electric energy prices and customers' demand. Since this model is based on expected mean input data (for an average day) and it is formalized as linear programming (that may require, for real cases, computation times of hours, as shown in Section 4.2), it is suitable for preliminary assessment on average daily V2G profitability. Therefore, the proposed model is to be considered particularly useful for defining strategies of CSSs companies and is not appropriate to be applied every day or dynamically during the day. For large-scale networks with day by day and/or real-time CSS and V2G management, implementing a heuristic/meta-heuristic algorithm would be required but this is beyond the scope of this work.

3. The proposed MILP model for the optimal fleet management of electric car-sharing systems with vehicle-to-grid operations

In this section, we describe the proposed Mixed Integer Linear Programming (MILP) model for optimal fleet and smart charging/discharging management of a one-way electric CSS. After a list of notations used in this paper (Section 3.1), in Section 3.2, we introduce the basic assumptions of the model and the description of the two KPIs (CSS revenues and V2G profits) used in the MILP objective function. Finally, in Section 3.3 we show in detail the MILP mathematical formulation.

3.1. Notation

This section summarizes all the mathematical notations and symbols adopted in the paper. They are grouped into three main categories: sets, matrices, and vectors, decision variables, and parameters used for solving the proposed model.

3.1.1. Sets, matrices, and vectors

$\boldsymbol{S} = \{1, \ldots, i, \ldots, S\}$: set of stations.
$\boldsymbol{T} = \{1, \ldots, t_s, \ldots, t_e, \ldots, T\}$: set of daily time steps.
$\boldsymbol{V} = \{1, \ldots, v, \ldots, V\}$: set of electric vehicles.
$\boldsymbol{A} = \{1_1, \ldots, i_{t-1}, i_t, i_{t+1} \ldots, S_T\}$: set of time-space network nodes obtained combining set $\boldsymbol{S}$ with set $\boldsymbol{T}$ with elements i_t representing station i at time step t.
$\boldsymbol{K} = \{1, \ldots, k, \ldots, K\}$: set of discretized intervals adopted for the piecewise linearization of the EV SOC charging/discharging pattern.
$\boldsymbol{C}$: time-space mean expected customer demand matrix with elements $c_{i,j}$ representing the number of customers leaving from origin i at time step t headed toward destination j with $i_t \in \boldsymbol{A}$, $j \in \boldsymbol{S}$.
$\boldsymbol{Z}$: parking places vector with elements z_i representing the number of parking places for each station $i \in \boldsymbol{S}$.
$\boldsymbol{\Delta}$: travel time matrix with elements δ_{ij} representing the number of time steps required to travel from origin i to destination j.
$\boldsymbol{e}$: mean expected electric energy unit price vector with elements, e_t representing the unit price at time step t.

3.1.2. Decision variables

$b_{i_t}^v$: binary decision variable which is 1 when vehicle $v \in \boldsymbol{V}$ parked at station $i \in \boldsymbol{S}$ is charging during time step $t \in \boldsymbol{T}$, and 0 otherwise.
$s_{i_t}^v$: binary decision variable which is 1 when vehicle $v \in \boldsymbol{V}$ parked at station $i \in \boldsymbol{S}$ is discharging during time step $t \in \boldsymbol{T}$, and 0 otherwise.
$w_{i_t}^v$: binary decision variable which is 1 when vehicle $v \in \boldsymbol{V}$, parked at station $i \in \boldsymbol{S}$, is on stand-by during time step $t \in \boldsymbol{T}$, and 0 otherwise.
$x_{i_t j}^v$: binary decision variable which is 1 when vehicle $v \in \boldsymbol{V}$ goes through arc $l = (i_t, j)$ from station $i \in \boldsymbol{S}$ to station $j \in \boldsymbol{S}$ at time step $t \in \boldsymbol{T}$, and 0 otherwise.
λ_k^{vt}: binary decision variable indicating the interval $k \in \boldsymbol{K}$ of the SOC of vehicle $v \in \boldsymbol{V}$ at time step $t \in \boldsymbol{T}$.
λb_k^{vt}: binary decision variable indicating the interval $k \in \boldsymbol{K}$ of the SOC of vehicle $v \in \boldsymbol{V}$ at time step $t \in \boldsymbol{T}$ during the charging process.
λs_k^{vt}: binary decision variable indicating the interval $k \in \boldsymbol{K}$ of the SOC of vehicle $v \in \boldsymbol{V}$ at time step $t \in \boldsymbol{T}$ during the discharging process.
SOC_t^v: non-negative decision variable indicating the battery SOC, in percentage, of vehicle $v \in \boldsymbol{V}$ at time step $t \in \boldsymbol{T}$.

3.1.3. Parameters

Q: battery energy capacity, expressed in kWh.
β_c^k: charging energy rate for interval $k \in \boldsymbol{K}$, in percentage, i.e., the amount of SOC increase per time step of the charging phase.

β_d^k: discharging energy rate for interval $k \in \boldsymbol{K}$, in percentage, i.e., the amount of SOC decrease per time step of the discharging phase.
ε_c: energy transfer efficiency during the charging phase, expressed in percentage.
ε_d: energy transfer efficiency during the discharging phase, expressed in percentage.
γ_c^k: transferred energy for the interval $k \in \boldsymbol{K}$, in kWh per time step of the charging phase, i.e., the amount of electric energy transferred from power grid to EV battery during a time step of the charging phase, with $\gamma_c^k = Q \cdot \beta_c^k \cdot \varepsilon_c$.
γ_d^k: transferred energy for the interval $k \in \boldsymbol{K}$, in kWh per time step of the discharging phase, i.e., the amount of electric energy transferred from EV battery to power grid during a time step of the discharging phase, with $\gamma_d^k = Q \cdot \beta_d^k \cdot \varepsilon_d$.
α: en-route battery discharging rate, in percentage, i.e., the amount of battery SOC decrease during a time step of a user trip.
p: EV usage fee per time step.
t_s: start of operating time step.
t_e: end of operating time step.
SOC_{min}: battery SOC minimum value (in percentage).
SOC_{max}: battery SOC maximum value (in percentage).

3.2. Model description and assumptions

In this section, we present how we modeled CSS operations, EV's charge/discharge phases, and the main problem parameters. The one-way station-based electric CSS consists of a set of CSS stations $\boldsymbol{S}$ and a set of electric vehicles $\boldsymbol{V}$. Each station $i \in \boldsymbol{S}$ has a number of parking places equal to z_i and is equipped with V2G-enabled charging columns so that one EV per parking place can be plugged in. The position and number of stations, the number of parking places for each station, and the number of vehicles are considered fixed input variables. Furthermore, we assume that the position and number of stations, as well as the number of parking places, EVs, and charging columns have been adequately designed for satisfying the current and the future customer demand.

We apply a time discretization by dividing the whole day into T time steps, considering $\boldsymbol{T}$ as the set of all time steps t included in a day. Each electric vehicle $v \in \boldsymbol{V}$ has a battery energy capacity Q and can be picked-up or returned by a customer to one of the $S = |\boldsymbol{S}|$ stations through a reservation-based system. Each day is divided into two time windows (see Fig. 1) named 'operating time' (from $t = t_s$ to $t = t_e$) and 'non-operating time' (rest of the day).

EVs must be booked in advance and used only during the operating time. Each vehicle $v \in \boldsymbol{V}$ can be in one of two states defined as 'inactive state' and 'active state' during the day. In the inactive states, EVs remain plugged into charging columns and are unused by customers; in the active states, EVs are unplugged from charging columns and are used by customers. In particular, inactive states can occur at any time of the day, while the active ones can happen only during the operating time.

The active state is the one that may generate CSS revenues. We consider a time-space network and a time-space matrix of customer demand for evaluating EVs trips between origin/destination stations during the active state. The time-space network is a directed graph where $\boldsymbol{A}$ is the set of all time-space nodes i_t obtained by combining the stations in set $\boldsymbol{S}$ with the time steps in set $\boldsymbol{T}$. In order to make a trip, the required information from the proposed model is related to customer demand. We set the time-space mean expected matrix of customer demand as matrix $\boldsymbol{C}$ with $c_{i,j}$ elements containing time and space information (origin station i, destination station j, and time step t at which customers wish to reserve an EV parked in the station i). In particular, during a trip made by a customer, an EV is moving in the time-space

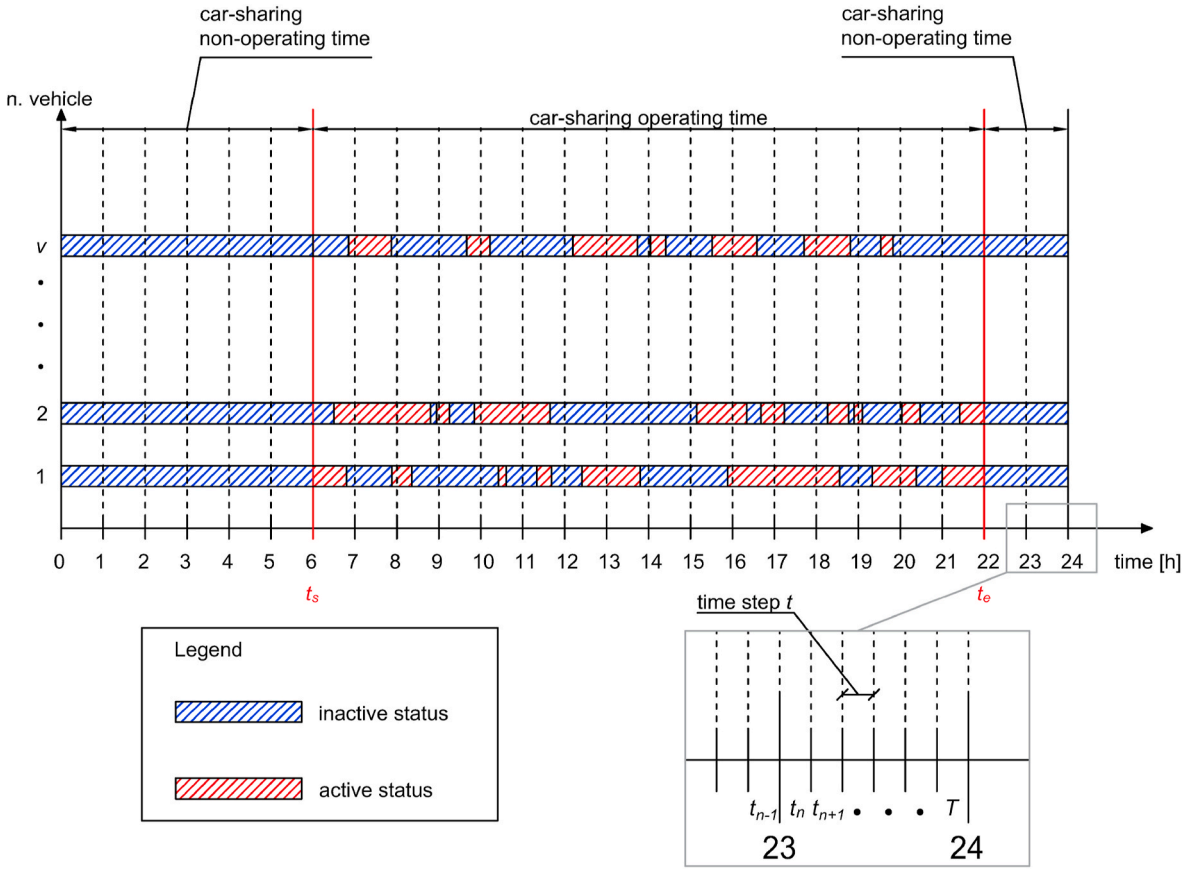

Fig. 1. The CSS operating scheme that is used in the proposed model.

network through arcs $l = (i_t, j)$. A vehicle v traverses an arc l according to the value of the decision variables $x^v_{i_t j}$. These variables assume a value equal to one if the arc l is traversed and a value equal to zero otherwise. The optimal distribution of the EVs at the beginning of the day ($t = 1$) is the first of the two model outputs. In particular, the optimal start-of-day station i for each vehicle v is the one where $\sum_{j \in \boldsymbol{S}} x^v_{i_1 j} = 1$. This EVs distribution has to be achieved through a static relocation (operator-based). In our model, the EVs transfers to be carried out through relocation, i.e., the planning of relocation staff operations, are not considered/suggested. To evaluate travel times, it is necessary to set the matrix Δ with elements δ_{ij} denoting the origin/destination travel time matrix between two nodes. The elements δ_{ij} represent the number of time steps needed to traverse arc $l = (i_t, j)$ at any time step t. Finally, we consider a fixed en-route battery discharging rate α that represents the amount of energy consumption during a time step of driving. CSS revenues are evaluated by multiplying the CSS fee p by the total driving time steps with clients.

The inactive state is the one that may generate V2G profits. During the inactive state, the batteries may be in one of the following phases: charging, discharging, and stand-by phase. Generally, the EV battery charging/discharging pattern is non-linear. For example, the charging function is divided into two phases: the first phase in which the charging rate is approximately linear in time and the second phase in which the charging rate is concave with time (Montoya et al., 2017). The EV battery charging functions applied in mathematical formulations, e.g., for solving EV routing problems, are divided into three groups, such as constant (Hof et al., 2017), linear (Hiermann et al., 2016), and non-linear charging functions (Montoya et al., 2017). A compromise between approximating the charging function and the computation time needed to solve the mathematical formulation may be assuming a piecewise linear charging function (Fu and Dong, 2019; Jamshidi et al., 2021) in which the charging pattern is divided into a certain number of intervals. Therefore, in the proposed model (see the M_PL model in section 3.3), we used a piecewise linear charging/discharging function considering a homogeneous discretization in K intervals. The charging and discharging rates are considered constant parameters when the EV battery SOC of vehicle v at time step t is in the k-*th* SOC interval but they are different for each interval. Under this assumption, in the charging phase, the battery state-of-charge SOC^v_t of vehicle v at time step t and interval k is increased by a rate β^k_c. Considering a charging energy transfer efficiency equal to ε_c, electric energy, in the interval k, γ^k_c (with $\gamma^k_c = Q \cdot \beta^k_c \cdot \varepsilon_c$) is purchased from the smart grid, during time step t, at mean expected energy unit price e_t. In the discharging phase, the reverse process occurs, i.e., the battery SOC^v_t is decreased by a rate β^k_d for vehicle v, time step t and interval k. Here, with a discharging energy transfer efficiency equal to ε_d, energy γ^k_d (with $\gamma^k_d = Q\,\beta^k_d \cdot \varepsilon_d$) is sold at an expected electric energy unit price e_t during time step t and transferred from the battery to the smart grid.

In the stand-by phase, there is no energy transfer (no purchase/sale occurs), and the SOC^v_t remains unchanged. Furthermore, the SOC for each vehicle v at the start-of-day is represented by the decision variables SOC^v_1. The proposed optimization model acts as a smart EVs charging/discharging management system, and these three phases, related to CSS EVs during a day, represent the second output of the proposed model. Therefore, for each vehicle v, station i, and time step t, charging, discharging, and stand-by phases are represented by binary decision variables named $b^v_{i_t}$, $s^v_{i_t}$, and $w^v_{i_t}$, respectively. These variables assume a value equal to one if the corresponding phase is in progress and a value equal to zero otherwise. V2G profits are given by the difference between energy sale revenues and energy purchase costs. V2G revenues, deriving from a vehicle v, are the sum, for all time steps, of the product of mean expected energy unit price e_t, transferred energy γ^k_c, and the decision variable $s^v_{i_t}$. Similarly, V2G costs, deriving from a vehicle v, are the sum, for all time steps, of the product of mean expected energy unit price e_t, transferred energy γ^k_d, and the decision variable $b^v_{i_t}$. V2G increases the number of battery charge/discharge cycles and could accelerate EV battery degradation (Dubarry et al., 2017). Indeed, the battery lifetime may depend on several factors such as temperature, time, charge/discharge cycles number and power rates, depth of discharge, battery SOC charging/discharging interval, capacity, C-rate, and previous degradation rate (Bishop et al., 2013; Rezvanizaniani et al., 2014; Pelletier et al., 2017; Thompson, 2018). However, in the literature, studies on the impact of V2G on batteries have shown variable results and there are conflicting opinions regarding this aspect (Lunz et al., 2012; Uddin et al., 2018). For example, Uddin et al. (2017) have demonstrated that extending EV Li-ion batteries lifetime through a smart grid algorithm is possible. For a review on V2G batteries capacity losses, see Noel et al. (2019). The proposition of a smart grid algorithm for managing battery lifetime in a CSS with V2G technology is beyond the scope of this work. Therefore, aspects related to battery degradation have not been considered.

3.3. Mathematical formulation

In this section, we describe the mathematical formulation of the proposed Mixed Integer Linear Programming (MILP) to optimize the EVs charging/discharging schedules and the start-of-day EVs distribution of a one-way station-based V2G electric CSS. The MILP formulation, named M_PL, is introduced as follows.

M_PL:

$$\max p \sum_{v \in \boldsymbol{V}} \sum_{i_t \in \boldsymbol{A}} \sum_{j \in \boldsymbol{S}} x^v_{i_t j} \cdot \delta_{ij} + \sum_{v \in \boldsymbol{V}} \sum_{i_t \in \boldsymbol{A}} \sum_{k \in \boldsymbol{K}} \left(e_t \cdot \gamma^k_d \cdot \lambda s^{vt}_k - e_t \cdot \gamma^k_c \cdot \lambda b^{vt}_k \right) \tag{1}$$

Subject to

$$\sum_{i \in \boldsymbol{S}} \sum_{j \in \boldsymbol{S}} x^v_{i_1 j} = 1, \forall v \in \boldsymbol{V} \tag{2}$$

$$\sum_{v \in \boldsymbol{V}} x^v_{i_t j} \leq c_{i_t j}, \forall\, i_t \in A, \forall j \in S,\ i \neq j \tag{3}$$

$$\sum_{j \in \boldsymbol{S}} x^v_{i_t j} = \sum_{j_{t-\delta_{ji}} \in \boldsymbol{A} \,|\, j \neq i} x^v_{j_{t-\delta_{ji}} i} + x^v_{i_{t-1} i}, \forall v \in \boldsymbol{V},\ \forall i_t \in \boldsymbol{A} \tag{4}$$

$$\sum_{v \in \boldsymbol{V}} \sum_{j \in \boldsymbol{S}} x^v_{i_t j} \leq z_i, \forall i_t \in \boldsymbol{A} \tag{5}$$

$$SOC^v_t = SOC^v_{t-1} + \varepsilon_c \cdot \sum_{k \in \boldsymbol{K}} \lambda b^{vt}_k \cdot \beta^k_c - \varepsilon_d \cdot \sum_{k \in \boldsymbol{K}} \lambda s^{vt}_k \cdot \beta^k_d - \alpha \sum_{i \in \boldsymbol{S} | i_t \in \boldsymbol{A}} \sum_{j \in \boldsymbol{S} | j \neq i} x^v_{i_t j} \cdot \delta_{ij}\ \forall v \in \boldsymbol{V},\ \forall t \in \boldsymbol{T} \tag{6}$$

$$b^v_{i_t} + s^v_{i_t} + w^v_{i_t} = x^v_{i_t i}, \forall i_t \in \boldsymbol{A},\ \forall v \in \boldsymbol{V} \tag{7}$$

$$SOC^v_1 \leq SOC^v_T,\ \forall v \in V \tag{8}$$

$$SOC_{min} \leq SOC^v_t \leq SOC_{max},\ \forall v \in V,\ \forall t \in T \tag{9}$$

$$\sum_{k \in \boldsymbol{K}} \lambda^{vt}_k \cdot \frac{100}{K} \cdot (k-1) \leq SOC^v_{t-1} \leq \sum_{k \in \boldsymbol{K}} \lambda^{vt}_k \cdot \frac{100}{K} \cdot k,\ \forall v \in V,\ \forall t \in T \tag{10}$$

$$\sum_{k \in \boldsymbol{K}} \lambda^{vt}_k = 1, \forall v \in \boldsymbol{V},\ \forall t \in \boldsymbol{T} \tag{11}$$

$$\sum_{k \in \boldsymbol{K}} \lambda b^{vt}_k = \sum_{i \in \boldsymbol{S} | i_t \in \boldsymbol{A}} b^v_{i_t},\ \forall v \in V,\ \forall t \in T \tag{12}$$

$$\sum_{k \in \boldsymbol{K}} \lambda s^{vt}_k = \sum_{i \in \boldsymbol{S} | i_t \in \boldsymbol{A}} s^v_{i_t},\ \forall v \in V,\ \forall t \in T \tag{13}$$

$$\lambda b_k^{vt} + \lambda s_k^{vt} \le \lambda_k^{vt},\ \forall v \in V,\ \forall t \in T, \forall k \in K \tag{14}$$

$$b_{i_t}^v,\ s_{i_t}^v, w_{i_t}^v \in \{0,1\}, \forall v \in V, \forall i_t \in A \tag{15}$$

$$x_{i,j}^v \in \{0,1\},\ \forall i_t \in A, \forall j \in S\ ,\ v \in V \tag{16}$$

$$\lambda_k^{vt}, \lambda b_k^{vt}, \lambda s_k^{vt}\ \in \{0,1\}, \forall v \in V,\ \forall t \in T, k \in K \tag{17}$$

The proposed M_PL model (1)–(17) aims to maximize the objective function (1), which is the sum of two terms. The first one (i.e., 'CSS revenues KPI') is the sum of the revenues obtained from the CSS customers' trips fee p. The second one (i.e., 'V2G profits KPI') is the sum of the profits resulting from the energy sale/purchase between EVs batteries and the power grid. The profits depend on the mean energy unit price e_t which is a function of time step t.

The objective function is subject to the following constraints. Constraints (2) guarantee that, at the start of the day ($t = 1$), each vehicle v can choose only one arc $l = (i_1, j)$ from station i to station j. It allows the start-of-day EV assignment at each station i. These constraints make no distinction between operating time and non-operating time. For this reason, it is necessary to introduce Constraints (3) which allow the EV assignment according to the requests of customers $c_{i,j}$ that leave from station i at time step t to reach destination j. To set the operating time range, the reservation system allows customers' requests $c_{i,j}$ only within two fixed time steps i.e., the starting operating time step t_s and the ending operating time step t_e. Furthermore, we set i not equal to j to avoid the wrong assignment of decision variables $x_{i,j}^v$ due to the null value of $c_{i_t i}$. Constraints (4) represent the continuity of flow constraints at each time-space node i_t. Constraints (5) define the capacity limit of each station i. Thus, the total number of EVs present at station i at time step t cannot exceed the maximum number of parking places z_i at this station. Constraints (6)–(10) define the variables, SOC_t^v, which represent the EV battery SOC of vehicle v at time step t. Specifically, Constraints (6) allow calculating the EV battery SOC at time step t by the residual SOC at the previous time step ($t-1$) and the sum of three terms. The first and the second term refer to the inactive state, while the third term refers to the active state, i.e., the electric energy consumption due to EVs displacement during CSS use. In particular, the first term provides the energy purchase from the power grid to the EVs batteries, while the second term provides the energy sale from the EVs batteries to the power grid. Constraints (7) ensure that only one of the charging, discharging, and stand-by phases are chosen during the inactive state of a vehicle v. Namely, when $x_{i_t i}^v = 1$, i.e., vehicle v is plugged into a charging column of station i during time step t, which means that only one of the three decision variables, $s_{i_t}^v$, $b_{i_t}^v$, and $w_{i_t}^v$ can be equal to one. Constraints (8) define the initial SOC of each vehicle v at time step $t = 1$. It must be lower than or equal to the SOC of the same vehicle v at the end of the day ($t = T$). Without these constraints, in order to obtain high V2G profits, the model would assign to SOC_1^v the maximum value allowed (e.g., SOC_{max}), arriving at the end of the day with the lowest possible SOC_T^v value (e.g., SOC_{min}). This behavior could be effective for one day, but it would not express the average operations of the system. Constraints (9) define the SOC lower bound and upper bound of all EVs for each time step t. Constraints (10) define the interval k in which the SOC of vehicle v at time step t belongs due to the binary decision variable λ_k^{vt}. Constraints (11) ensure that exactly one interval k is selected for each vehicle v at each time step t. Constraints (12)–(13) allow assigning the binary decision variables λb_k^{vt} and λs_k^{vt} through the binary decision variables $b_{i_t}^v$ and $s_{i_t}^v$ during the charging/discharging phases, respectively. Constraints (14) ensure for each vehicle v and time step t that at most one decision variable between λb_k^{vt} and λs_k^{vt} can be equal to 1 if the corresponding variable λ_k^{vt} is equal to 1. Finally, Constraints (15)–(17) define the domain of the decision variables.

Solving problem (1)-(17) results in two main outputs, namely the EVs charging/discharging schedule, expressed by the optimal values of $b_{i_t}^v$, $s_{i_t}^v$ and $w_{i_t}^v$, including the SOC at the start of the operating time (SOC_1^v), and the start-of-day EVs distribution among stations according to the values of decision variables $x_{i_1 j}^v$.

The proposed M_PL model (1)–(17) can be reformulated considering the EV charging/discharging energy rates as constant during the whole phase and for every EV battery SOC ($\gamma_c^k = \gamma_c$; $\gamma_d^k = \gamma_d$; $\beta_c^k = \beta_c$; $\beta_d^k = \beta_d$). In other words, this simplification could consistently decrease the number of decision variables and, consequently, improve the performance of the proposed model. Thus, the M_PL model can be reformulated in the M_C model as follows.

M_C:

$$\max\ p\sum_{v\in \boldsymbol{V}}\sum_{i_t\in \boldsymbol{A}}\sum_{j\in \boldsymbol{S}} x_{i,j}^v \cdot\ \delta_{ij}\ + \sum_{v\in \boldsymbol{V}}\sum_{i_t\in \boldsymbol{A}}\left(e_t \cdot\ \gamma_d \cdot\ s_{i_t}^v - e_t \cdot\ \gamma_c \cdot\ b_{i_t}^v\right) \tag{18}$$

Subject to

$$\sum_{i\in \boldsymbol{S}}\sum_{j\in \boldsymbol{S}} x_{i_1 j}^v = 1, \forall v \in \boldsymbol{V} \tag{19}$$

$$\sum_{v\in \boldsymbol{V}} x_{i,j}^v \le\ c_{i,j}, \forall\ i_t \in A, \forall j \in S,\ i \ne j \tag{20}$$

$$\sum_{j\in \boldsymbol{S}} x_{i,j}^v = \sum_{j_{t-\delta_{ji}}\in \boldsymbol{A}\,\middle|\, j\ne i} x_{j_{t-\delta_{ji}} i}^v + x_{i_{t-1} i}^v, \forall v \in \boldsymbol{V},\ \forall i_t \in \boldsymbol{A} \tag{21}$$

$$\sum_{v\in \boldsymbol{V}}\sum_{j\in \boldsymbol{S}} x_{i,j}^v \le z_i, \forall i_t \in \boldsymbol{A} \tag{22}$$

$$SOC_t^v = SOC_{t-1}^v + \varepsilon_c \cdot \beta_c \sum_{i\in \boldsymbol{S}|i_t\in \boldsymbol{A}} b_{i_t}^v - \varepsilon_d \cdot \beta_d \sum_{i\in \boldsymbol{S}|i_t\in \boldsymbol{A}} s_{i_t}^v - \alpha \sum_{i\in \boldsymbol{S}|i_t\in \boldsymbol{A}}\sum_{j\in \boldsymbol{S}|j\ne i} x_{i,j}^v \cdot \delta_{ij}\ \forall v \in \boldsymbol{V},\ \forall t \in \boldsymbol{T} \tag{23}$$

$$b_{i_t}^v + s_{i_t}^v + w_{i_t}^v = x_{i_t i}^v, \forall i_t \in \boldsymbol{A}, \forall i \in \boldsymbol{S},\ \forall v \in \boldsymbol{V} \tag{24}$$

$$SOC_1^v \le SOC_T^v,\ \forall v \in V \tag{25}$$

$$SOC_{min} \le SOC_t^v \le SOC_{max},\ \forall v \in V,\ \forall t \in T \tag{26}$$

$$b_{i_t}^v,\ s_{i_t}^v, w_{i_t}^v \in \{0,1\}, \forall v \in V, \forall i_t \in A \tag{27}$$

$$x_{i,j}^v \in \{0,1\},\ \forall i_t \in A, \forall j \in S,\ v \in V \tag{28}$$

The comparison between the proposed M_PL model and its reformulation (M_C model) is shown in Section 4.1.

4. Numerical application

To test the proposed model effectiveness, we applied it on a small-size (Section 4.1) and a real-size network (Section 4.2) for evaluating mean car-sharing system revenues and V2G impacts/profitability. Besides, for the real case network, a sensitivity analysis is carried out tuning up different parameters. As a result of the proposed model scenario, referred to as 'V2G-CSS' from now on, it is possible to provide the optimal EV charging/discharging schedule and the optimal day-ahead assignment of EVs at each station at the beginning of the day, considering a fixed EV fleet and a fixed mean expected demand.

4.1. Small-size numerical application

In this section, we tested the M_PL model and its reformulation in order to evaluate their behavior in terms of objective function, number of decision variables, and computation time.

The test network of this small-size application has the following characteristics: the total number of stations is set equal to 5 ($S = 5$) with 5 parking places each ($z_i = 5$ for each station $i \in S$). The EV fleet consists

of 10 EVs ($V = 10$) and the operating time is set equal to 10 h ($T = 10$) from 2:00 p.m. to 11:00 p.m. In this test, the non-operating time is not considered, that is $t_s = 1$ and $t_e = T$. The operating time was discretized into 10 time steps of 1 h. Mean electric energy unit price e_t varies between 0.05 €/kWh and 0.25 €/kWh, following a typical day-ahead electricity market trend (see Fig. 5). The car-sharing usage fee per time step is set equal to $p = 15$ €/h (i.e., 0.25 € per minute). All the stations are equipped with fast-charging columns with CHAdeMO connectors enabled with V2G technology. CHAdeMO is a Direct Current (DC) charging protocol developed by CHAdeMO Association. This protocol currently enables EV charging from 6 kW to 400 kW (CHAdeMO Association, 2021). The EV model chosen for this application is the Nissan Leaf, 2019 with a battery capacity of $Q = 40$ kWh, equipped with two inlets (Type 2 Alternating Current (AC) and CHAdeMO) and enabled with bidirectional charging. Considering the features of this EV model (Nissan Leaf, 2019), we assumed that the maximum vehicle range equals 270 km and the full-charge time (from 0% to 100% of EV battery SOC) equals 135 min. We set the EV average travel speed equal to 25 km/h. The en-route battery discharging rate per time step is equal to $\alpha = 9.26\%$. This value is calculated considering the ratio between EV maximum covered distance and the EV average travel speed for each time step. Finally, the travel time matrix Δ and the time-space mean expected demand are shown in Table 1 and Table 2, respectively. We highlight that the inputs used for numerical applications do not contain users' private information in order to follow privacy policies. Therefore, in Table 2, we consider customers' movements through an identification number named 'Customer ID'.

We tested the M_PL model with a piecewise linear function discretizing the non-linear charging pattern of EV SOC through K intervals. Considering a Nissan Leaf 40 kW DC non-linear fast charge pattern (Fastned, 2021), we discretized it with a piecewise linear function through 5 intervals ($K = 5$), with the following EV SOC ranges (in percentage): [0, 20), [20, 40), [40, 60), [60, 80), and [80, 100]. From the SOC-Power graph, we obtained the corresponding SOC-time graph (Fig. 2) considering 1 h time steps with the following EV charge time ranges (in minutes): [0, 60), [20, 80], [40, 100), [60, 120), and [75, 135].

From the SOC-time graph, we obtained the corresponding charging rates β_c^k for each *k-th* interval, where $\beta_c^1 = 57.03\%$, $\beta_c^2 = 54.93\%$, $\beta_c^3 = 47.49\%$, $\beta_c^4 = 36.51\%$, and $\beta_c^5 = 30.62\%$. Hence, charging rates β_c^k are the average values between the minimum and maximum values of the *k-th* interval range. According to equation $\gamma_c^k = Q \cdot \beta_c^k \cdot \varepsilon_c$, we obtained also the corresponding transferred energy during the charging process γ_c^k, where $\gamma_c^1 = 20.53$ kWh, $\gamma_c^2 = 19.77$ kWh, $\gamma_c^3 = 17.10$ kWh, $\gamma_c^4 = 13.14$ kWh, and $\gamma_c^5 = 11.02$ kWh. Due to the lack of data availability for Nissan Leaf discharging pattern, we set for this case the charging rate $\beta_d^k = 44.40\%$ and the transferred energy $\gamma_d^k = 16$ kWh considered as constants for all *k-th* intervals.

We solved the proposed M_PL model on a cluster of two computers using the CPLEX MILP exact solver of IBM ILOG. The two computers consist of 2 CPU Intel Xeon(R) E5-2660 v3 3.3 GHz, 10 cores (20 logical processors), and 128 GB memory each. Due to IBM LOG software limitations, only 16 cores (32 logical processors) have been used.

Table 1
Travel time matrix Δ expressed as the number of time steps t (hours) needed to travel from station i to station j.

Origin station i	Destination station j				
	1	2	3	4	5
1	0	1	2	3	2
2	1	0	1	2	3
3	2	1	0	1	3
4	3	2	1	0	2
5	2	3	3	2	0

Table 2
Time-space mean expected demand.

Customer ID	Origin i	Destination j	Origin of the trip time step t
1	1	2	2
2	2	5	5
3	3	4	7
4	3	5	7
5	3	1	7
6	4	5	1
7	5	1	4
8	5	1	5

We run the model without CPU time limit and with a relative gap tolerance equal to 0%. The relative gap tolerance is the relative difference between the upper bound on the optimal objective function value (UB) and the lower bound (LB), i.e., the best-found objective function value, and it is calculated as $\frac{UB-LB}{UB} \times 100$ expressed in percentage. With these settings, the optimization was not successful since the maximum available memory has been reached. Indeed, we set the CPU time limit equal to 72 h obtaining the following results with 1.48% of relative gap tolerance. The sum of V2G profits and V2G-CSS revenues (objective function value) is equal to 278.1 €. In particular, 'CSS revenues KPI' is equal to 240 € and 'V2G profits KPI', namely the difference between energy sale revenues and energy purchase costs is equal to 38.1 €. Since optimality has not been reached (relative gap tolerance equal to 0%), we decided to deeply analyze the reformulation of the proposed model (M_C model) optimization. In this case, the charging and discharging energy rates per time step (1 h) are considered the same and equal to $\beta_c = \beta_d = 44.40\%$. Furthermore, considering $\varepsilon_c = \varepsilon_d = 90\%$, the transferred energy per time step is $\gamma_c = \gamma_d = 16$ kWh.

The obtained results can be compared with a baseline scenario of a car-sharing system without V2G operations, referred to as 'B_CSS'. In other words, in this scenario, it is only allowed to purchase energy from the grid (G2V) but not to sell it (the decision variables $s_{i_t}^v$ have been set equal to zero). The M_C model has been solved in a computation time equal to 2.3 s, and the main results are shown in Table 3.

From Table 3 we can observe that, for V2G-CSS, the optimal value of the objective function is equal to 277.6 €. In particular, 'CSS revenues KPI' is equal to 240 € (86.5% of the objective function) and 'V2G profits KPI', namely the difference between energy sale revenues and energy purchase costs is equal to 37.6 € (i.e., 13.5% of the objective function). Revenues for both scenarios are the same. However, the sale of energy in the proposed scenario allows not only to recover the required costs to charge the EVs, but also to obtain positive profits. Furthermore, V2G profits may be valued as revenues from car-sharing system usage. Since in this application the average revenue per user is equal to 30 €, V2G profits can be considered as the equivalent of about 1 more customer out of 8.

The solution can also be depicted on the time-space network of Fig. 3. In this figure, each time-space node i_t is represented by a circle and the number of EVs parked at station i at time step t is contained inside.

According to Constraints (19), (21), and (22), each vehicle v must move between time-space nodes depending on the values of $x_{i_t i}^v$ or $x_{i_t j}^v$. If $x_{i_t i}^v = 1$, it means that the EV is moving only through time and not through space, i.e., the EV remains parked at the same station between two consecutive time steps. On the contrary, if $x_{i_t j}^v = 1$, the EV is moving through the time-space arc $l = (i_t, j)$, and is used by a customer. As shown in Fig. 3, the EVs movements between time-space nodes are represented by two types of arrows. The blue and the red arrows display the decision variables $x_{i_t i}^v$ and $x_{i_t j}^v$, respectively. Furthermore, observing Table 2 and Fig. 3, we can see that all user demand is satisfied. In particular, three vehicles (vehicles 5, 6, and 8) are not used by customers, i.e., the V2G-CSS revenues coming from these vehicles are equal to zero (see Table 3).

The optimal energy sale/purchase scheduling for each EV, that is the vehicle-by-vehicle EV battery SOC for each time step, is shown in Fig. 4.

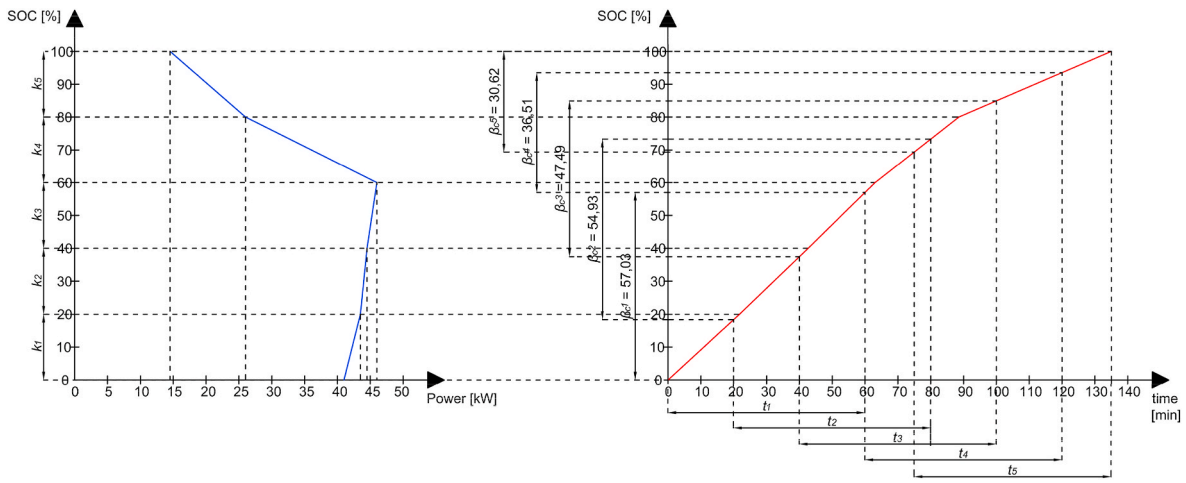

Fig. 2. SOC-Power and SOC-time graphs with piecewise linear charging function implemented in the M_PL model.

Table 3
Small-size application main results.

EV v	B_CSS			V2G-CSS				
	Start-of-day assigned station i	B_CSS revenues [€]	Energy purchase costs [€]	Start-of-day assigned station i	V2G-CSS revenues [€]	Energy sale revenues [€]	Energy purchase costs [€]	V2G profits [€]
1	1	60	−1.6	1	60	3.2	−3.2	0
2	2	0	0	3	15	8	−4	4
3	3	0	0	3	30	8	−4	4
4	3	15	−0.8	3	45	4.8	−2.4	2.4
5	3	30	−0.8	4	0	8	−2.4	5.6
6	3	45	−0.8	4	0	8	−2.4	5.6
7	4	30	0	4	30	7.2	−3.2	4
8	5	0	0	5	0	8	−2.4	5.6
9	5	30	−0.8	5	30	6.4	−4	2.4
10	5	30	−0.8	5	30	8	−4	4
	Total	**240**	**−5.6**		**240**	69.6	−32	**37.6**

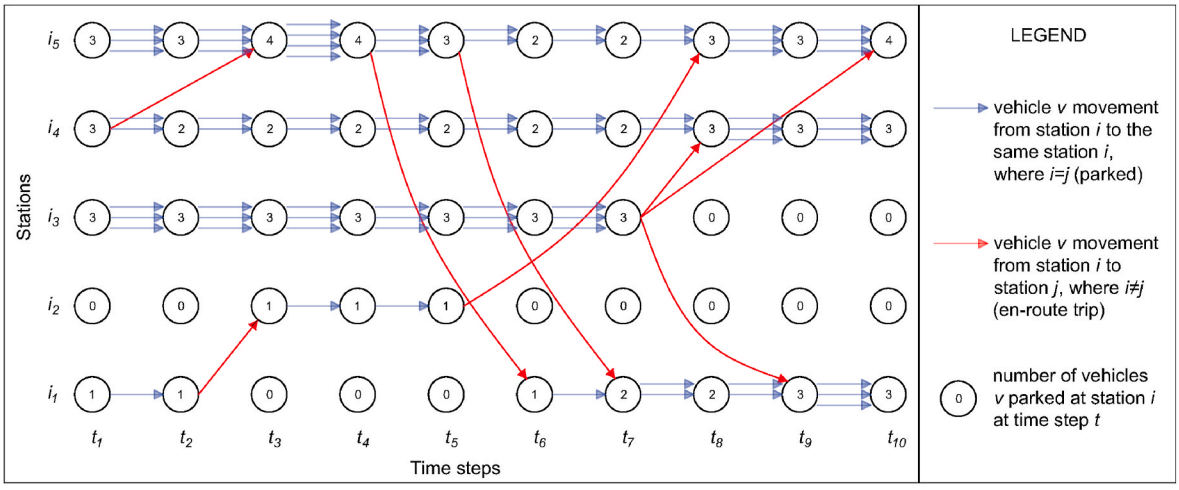

Fig. 3. Time-space network functioning scheme.

The charge phase is shown with solid lines, the discharge phase with dotted lines while the en-route discharge phase with dashed lines.

Except for vehicle 8 (which is one of the three vehicles not used by customers), we can see that the SOC of the EVs, at the beginning and the end of the operating time considered, take on values that are close to each other, i.e., about 20%–40% and about 30%–50%, respectively.

To better understand the trend of EVs SOC, it is useful to observe Fig. 5. This figure shows the total amount of energy transferred from EVs to the power grid, and vice versa, and the values of energy unit price during the day that were considered in this small-size numerical application.

The model allows smart charge/discharge operations, that is, it allows to purchase energy (charge phases) when the mean energy unit price e_t is low and to sell energy when e_t is high. In particular, 348 kWh are purchased from the power grid to charge the EVs batteries against 432 kWh sold from EVs batteries to the power grid.

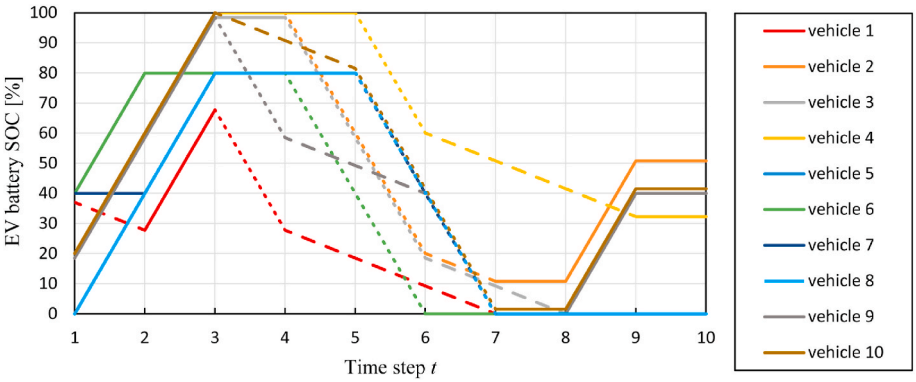

Fig. 4. Test network results: EV battery SOC variation for each time step.

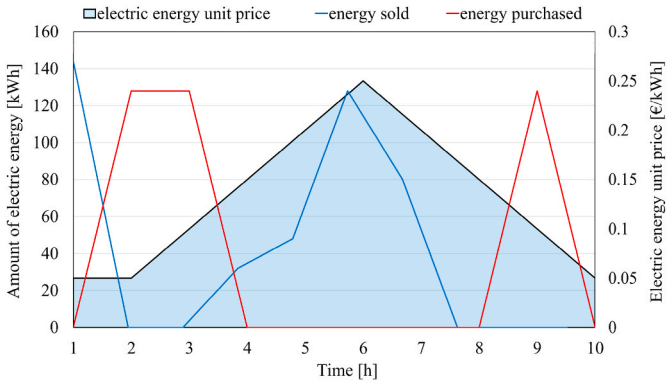

Fig. 5. The energy exchanged and energy unit price.

A comparison between the M_PL and M_C models in terms of the objective function, number of decision variables, and computation time is shown in Table 4a and Table 4b.

From Table 4a, we can observe that the objective functions differ by 0.5 €. From Table 4b, we can observe that for solving the small-size test network, the M_PL model has a much higher number of binary decision variables, non-zero coefficients, and constraints. Furthermore, the difference in terms of computation time between the M_PL and M_C models is not comparable (i.e., 2.3 s against 72 h) despite only 10 h of operating time having been considered. For this reason, the M_PL model turned out to be not applicable for large-size networks due to too high computation time. We can state that the M_C model is more appropriate to use in practice compared to the M_PL model since the difference in the objective function values is small and the computation time for the M_C model is only 2.3 s compared to 72 h for the M_PL model. It seems that the adoption of the EV charging/discharging constant function yielded similar V2G-CSS revenues and V2G profits when compared to EV charging/discharging piecewise linear function. Hence, the adoption of M_C model is not only convenient in terms of computation time but also acceptable in terms of the realism of the results in this context. Thus, for the large-size network (Section 4.2) the M_C model with constant EV charging/discharging function has been applied. Note that this is not to say that such simplification should always be done, we argue that for the purpose of understanding the scale of the economic benefits of V2G used as part of a car-sharing system.

4.2. *Real case network: the city of Delft*

The M_C model (18)–(28), also referred to as 'the proposed model' from now on, has been applied to the city of Delft, the Netherlands. The numerical application is a 'quasi-real' case study, because only a part of the data used is real. The real data comes from the Dutch mobility dataset (used by Correia and van Arem (2016), Liang et al. (2018), and Liang et al. (2020)) and the Delft road network. The Dutch government collects the mobility dataset for mobility research gathering daily information related to households' purposes of travel, origin and destination, transport mode, departure, and arrival times. The original dataset contains 68,640 trips made by Delft households during one day of the year 2008.

The dataset has been filtered and aggregated to obtain a mean hypothetical next day expected car-sharing demand among the Delft city zones. We have assumed that several CSSs operate in the city of Delft. Therefore, this demand should be satisfied by all CSSs in the city. According to the assumed CSSs operating time, set as 6:00 a.m. - 10:00 p.m., the total number of trips in the dataset using cars and taxis was reduced to 20,640. These trips have been aggregated into several groups, each consisting of households with the same characteristics, i.e.,

Table 4a
Objective function results comparison for the small-size test network - V2G-CSS scenario.

EV charging/discharging function	Obj. fun. value [€/day]	Obj. fun. Upper Bound [€/day]	Rel. gap [%]	V2G-CSS revenues KPI [€/day]	Energy sale revenues [€/day]	Energy purchase costs [€/day]	V2G profits KPI [€/day]
Piecewise linear function (M_PL)	278.1	282.2	1.48	240	72.8	34.7	38.1
Constant function (M_C)	277.6	277.6	0.00	240	69.6	32.0	37.6

Table 4b
Performance results comparison for the small-size test network - V2G-CSS scenario.

EV charging/discharging function	Decision variables		Non-zero Coeff.	Constr.	CPU time [s]
	Binary	Continuous			
Piecewise linear function (M_PL)	5680	100	23980	2700	260000
Constant function (M_C)	4000	100	18880	1700	2.3

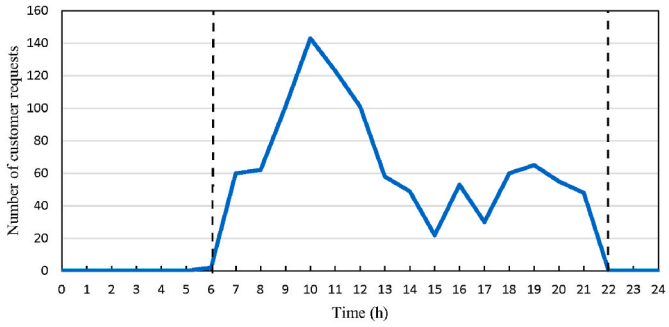

Fig. 6. CSS demand pattern.

gender, age, and education level. The total number of trips of each group has been divided by a coefficient $\mu = 20$ called expansion coefficient (Correia and van Arem, 2016), to consider only the fraction of the car-sharing demand. Therefore, for the 20,640 real households' trips, 1032 CSS trips have been considered in the model. This demand has been aggregated into 10-min intervals and shows the trend depicted in Fig. 6. Furthermore, in this numerical application, all CSS trips are assumed as booked in advance and the origin and destination, as well as the starting departure time, are obtained from the original database. The proposed model does not require knowing users' sensitive information. For more details, see the recent advanced model proposed by Li et al. (2021a) that considers users' privacy protection.

We assume that one of the CSSs operating in the city of Delft has V2G-enabled EVs and charging columns. We apply our proposed model to this system (V2G-CSS). We have set the number of car-sharing stations of this system equal to 19. These stations have been located by maximizing the V2G-CSS covered area and considering a customer catchment area of each station based on the maximum walking distance that a car-sharing customer can cover. This distance has been set equal to 500 m (Herrmann et al., 2014). By placing a V2G-CSS station in the center of a catchment area and considering Euclidean distances, a station can be reached from any point of a circle centered in the station and with a radius of 500 m. However, the city of Delft does not have a radial street network but approximately a grid street layout. For this reason, we have considered Manhattan distances according to the Taxicab geometry (Krause, 1973) instead of Euclidean distances. Therefore, the customer catchment area is not a circle, but a square centered in the station with the diagonals parallel to the streets and 1000 m long (taxicab circle). In Fig. 7, the V2G-CSS stations and the customer catchment areas are shown.

The trips dataset is defined according to the Origin/Destination (OD) demand matrix among 46 centroids (see black nodes in Fig. 7). However, it is assumed that all customers within the taxicab circle will use the car-sharing station located in the respective center. For this reason, a data aggregation process was used to define the V2G-CSS demand matrix $\boldsymbol{C}$. The OD V2G-CSS demand of the centroids falling in a taxicab circle, as well as the corresponding departure times, have been aggregated in the center of the circle. For example, station s_1 demand is the sum of centroids 1 and 24 demand. Some centroids (see red nodes of Fig. 7) do not present any customers' OD demand, so they have not been considered in the data aggregation process.

The travel time matrix Δ has been calculated by dividing the minimum distance between two stations along with the Delft street network by the average speed of an EV and by the duration of a time step. The shortest paths have been evaluated by applying Dijkstra's algorithm. We set an EV average speed equal to 15 km/h and a time step equal to 10 min. For example, the $\delta_{1,15}$ element of the travel time matrix (the travel time between station s_1 and s_{15}) is equal to 3 time steps since the distance between s_1 and s_{15} is equal to 7 km.

We assumed that each of the 19 stations distributed on the Delft network has 10 parking places available ($z_i = 10$ for each station $i \in \boldsymbol{S}$).

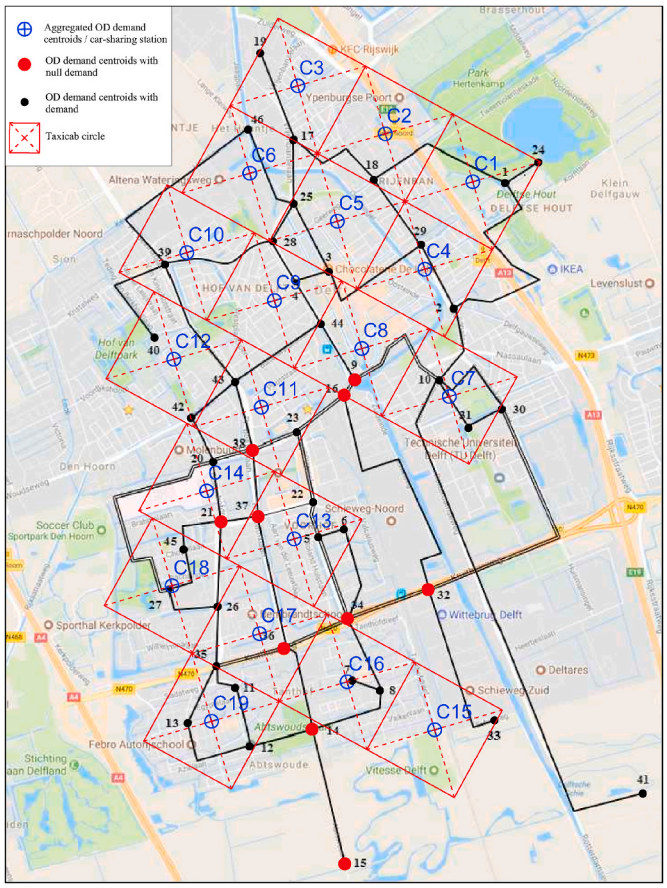

Fig. 7. Delft network and catchment areas (based on Maps Data: Google, ©2019).

The EV fleet consists of 50 EVs ($V = 50$) and the used EV car model is the same as in the small-size numerical application. Based on the mean expected demand, this system sizing was set to saturate the V2G-CSS usage, reducing the time the EVs are parked. In this way, the opportunities to sell/buy energy (i.e., to obtain V2G profits) are on average reduced. The whole day was divided into 144 time steps ($T = 144$), considering time steps t of 10 min. The operating time has been set equal to 16 h between $t_s = 36$ (6:00 a.m.) and $t_e = 132$ (10:00 p.m.) while the non-operating time is set equal to 8 h between $t = 1$ (00:10 a.m.) and $t_{s-1} = 35$ (05:50 a.m.), and from $t_{e+1} = 133$ (10:10 p.m.) to $T = 144$ (12:00 a.m.). The V2G-CSS usage fee per time step has been set equal to $p = 2.5$ €/time step.

Generally, the electric energy price is a time and day dependent variable due to the energy demand response trade. Several authors have

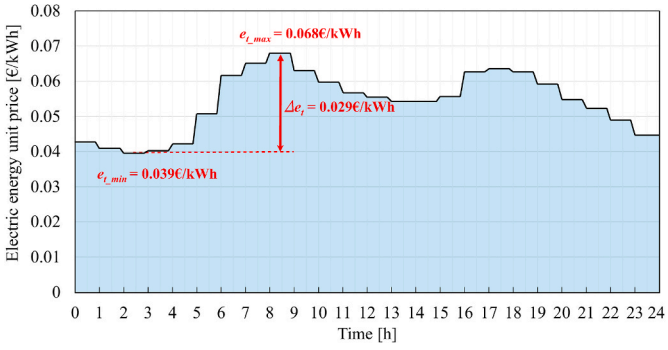

Fig. 8. Day-ahead Dutch electricity market: daily electric unit price variation – average values of a weekday of year 2018.

introduced prediction models for electric energy prices (Contreras et al., 2003; Shuman and Yang, 2019) and Jiang and Hu (2018) have recently written a review paper. We assume that the mean next-day expected energy prices can be obtained from the day-ahead electricity market. Specifically, we considered the average hourly electric energy prices of one typical weekday in 2018 obtained from the official day-ahead Dutch electricity market (SMARD, 2019) as depicted in Fig. 8. In particular, during the day, the electric energy unit price e_t varies between 0.039 €/kWh and 0.068 €/kWh. Notice as well that power in the city is modeled in an aggregated way meaning that we do not consider that the grid may be stronger or weaker in different parts of the city.

To perform a sensitivity analysis, two different types of V2G charging columns/speed (Level 2 with Alternating Current named L2, Level 3 with Direct Current (DC) fast charge named L3) and three different vehicle battery capacities ($Q1 = 24$ kWh, $Q2 = 40$ kWh, and $Q3 = 62$ kWh) have been considered. From the combination of the charging column types and the battery capacities, six scenarios were evaluated (L2Q1, L2Q2, L2Q3, L3Q1, L3Q2, L3Q3). For each of these scenarios, we have solved a corresponding baseline scenario (B_CSS) that is a car-sharing system without V2G operations (B_L2Q1, B_L2Q2, B_L2Q3, B_L3Q1, B_L3Q2, B_L3Q3). As assumed in the small-size numerical application for the M_C model, the charging and discharging energy rates, and consequently the transferred energy per time step, were considered the same for each scenario ($\beta = \beta_c = \beta_d$ and $\gamma = \gamma_c = \gamma_d$). However, two energy transfer efficiency ($\varepsilon = \varepsilon_c = \varepsilon_d = 95\%$ for L2 and $\varepsilon = \varepsilon_c = \varepsilon_d = 90\%$ for L3) have been considered. The six different scenarios with the corresponding parameter values (obtained as described in Section 3 and in the small-size numerical application) are shown in Table 5.

In order to obtain near-optimal solutions in reasonable computation time, we set the relative gap tolerance equal to 10% and the CPU time limit equal to 72 h.

4.2.1. Results analysis

The results of the proposed model scenarios (V2G-CSS) were obtained in a mean computation time equal to 28.4 h where L2Q1 is shown to be the fastest scenario solved (4 h) while L3Q1 the slowest one (see Table 6).

Computation times could be accelerated by using more recent/performing CPUs or increasing the relative gap tolerance. The satisfied demand and the average number of trips are very similar across all scenarios. In particular, for baseline/proposed model scenarios, the average satisfied demand and the average number of trips are equal to 28.5%/27.1% and 294/279, respectively. Indeed, for one-way CSSs, fully satisfy the demand requires a large number of vehicles to face odd trips, if there are no vehicle relocation operations during the day (Correia and Antunes, 2012). The rest of the demand is supposed to have been satisfied by the other car-sharing systems assumed to operate in the city of Delft. The main obtained results of all tests are shown in the next tables and figures. Specifically, Table 7a and Table 7b summarize the optimization results of the six baseline/proposed model scenarios in terms of objective function value, upper bound objective function value, relative gap, and KPIs. Table 8 and Fig. 9 summarize the V2G-CSS scenario results regarding energy transferred from/to the grid during the operating and non-operating time. Table 9 shows the number of EVs assigned through the optimization at the beginning of the day among all stations. Finally, Fig. 10 depicts the optimized daily EVs charging/discharging schedules for the main proposed model scenarios.

According to Tables 7a and 7b, we can make the following observations from an economic point of view:

- For the V2G-CSS scenarios, the average revenue is equal to 1510.05 €/day. This value appears to be lower than the baseline scenarios, but this revenue was obtained for higher average relative gaps (see L3Q2 case). The baseline solutions should also be feasible for V2G-CSS scenarios (no energy is sold) and so, optimal V2G-CSS solutions should always be better or the same. The higher upper bounds for V2G-CSS scenarios, compared to the corresponding baseline ones, indicate that there is indeed room to find better solutions. The average V2G profit is equal to 36.04 €/day, and it is comparable with those estimated by Khalen et al. (2018) and Fournier et al. (2014). The best results appear to be those of L3Q3 with the highest V2G profit corresponding to the highest V2G-CSS revenue. However, it is not possible to define the best scenario among the six with great certainty because the obtained objective function and KPI values are very similar to each other with different relative gaps.
- We can observe that V2G profits resulted to be much lower than CSS revenues in all scenarios. Since the value of the parameter p (usage fee per time step) has been set higher than any difference between two energy prices e_t, the priority of the optimization is to maximize the V2G-CSS use with respect to V2G profits. This implies that the sale of energy takes place mostly if it does not increase the unsatisfied demand. Hence, the V2G profits term does not negatively affect the CSS revenue term in the optimization. We can observe it by comparing B_L2Q2 and V2G_CSS L2Q2 scenarios results where we obtained the same amount of CSS revenues (1550 €/day) with a comparable relative gap (0.21% and 0.57%, respectively).
- If we look at the baseline scenarios, we can see that the charging costs are lower than the corresponding values of the V2G-CSS scenarios. Therefore, most of the charging costs are due to the profitability given by the purchase of energy at a lower price to be sold later at a higher price. Since the profits are positive in each scenario, the V2G technology also allows to fully cover the daily charging costs due to users' trips.
- In all scenarios (V2G-CSS and B_CSS), customers use EVs on average for only about 12% of the operating day. This value is comparable with the vehicles utilization rate evaluated by Sprei et al. (2019) over 12 European and US cities for free-floating CSS. Accordingly, for about 88% of a day, CSS EVs are parked and, consequently, do not generate any revenue for CSS companies. Given that V2G-CSS mean revenue per customer is equal to about 5.5 €, V2G profits can be considered equivalent to about 7 more customers out of 279 during a day.

From Table 8 and Fig. 9, we can make several key considerations, for the V2G-CSS scenarios, from an energy point of view:

- Considering the L2 charge speed type, the V2G-CSS could provide more than 1 MWh from 50 EVs during the operating time. Specifically, the best scenario in terms of net energy supplied to the grid

Table 5
Parameters used in the six scenarios.

Scenario	Charger type	Q [kWh]	β [%]	ε [%]	α [%]	γ [kWh]	Full-charge time [h]	Maximum range [km]
L2Q1	L2 (AC)	24	3.03	95	1.25	0.691	5.5	200
L2Q2	L2 (AC)	40	2.22	95	0.92	0.844	7.5	270
L2Q3	L2 (AC)	62	1.45	95	0.65	0.855	11.5	385
L3Q1	L3 (DC)	24	12.5	90	1.25	2.70	1.33	200
L3Q2	L3 (DC)	40	7.4	90	0.92	2.67	2.25	270
L3Q3	L3 (DC)	62	4.76	90	0.65	2.67	3.5	385

Table 6
Comparison between V2G-CSS and baseline CSS scenarios in terms of problem size and computation time.

Scenario	Decision variables		Non-zero Coeff.	Constr.	CPU time [h]					
	Binary	Continuous			L2Q1	L2Q2	L2Q3	L3Q1	L3Q2	L3Q3
V2G-CSS	3009600	7200	18691600	395483	4.02	28.27	13.81	56.84	50.03	17.63
B_CSS	2880000	7200	18281201	395483	0.79	0.78	0.74	0.37	0.55	0.50

Table 7a
Main baseline scenarios results.

B_CSS scenario	Obj. fun. value [€/day]	Obj. fun. Upper Bound [€/day]	Rel. gap [%]	B_CSS revenues KPI [€/day]	Energy purchase costs [€/day]	Average EVs usage [%]
B_L2Q1	1531.67	1550.10	1.20	1540.0	8.33	12.90
B_L2Q2	1545.13	1548.42	0.21	1550.0	9.87	13.10
B_L2Q3	1516.34	1547.57	2.06	1527.5	11.16	12.58
B_L3Q1	1530.05	1550.10	1.31	1540.0	9.95	12.79
B_L3Q2	1521.91	1548.40	1.74	1535.0	13.09	12.88
B_L3Q3	1545.19	1547.51	0.15	1557.5	12.31	12.79

during the operating time resulted to be scenario L2Q2 with around 1.6 MWh. For L3 charge speed type, the V2G-CSS could provide less than 1 MWh from 50 EVs during the operating time from scenario L3Q1. Aside from scenario L3Q1, from scenario L3Q2 and L3Q3, the amount of net energy provided to the grid during the operating time is around 1.6 and 2.3 MWh, respectively. In general, the net energy transferred to the grid during the operating time resulted to be significant. Considering an average energy demand per household of 10 kWh/day (see de Almeida et al., 2011), according to the results of all scenarios, during the energy peak hour period, each EV could satisfy around 2 households electric energy supply.

- The mean transferred energy from the grid to the vehicles of the baseline scenarios is much lower than that of the V2G-CSS scenarios (16% only). The greater the charging speed, the greater this difference. In other words, in the V2G-CSS scenarios, most of the energy purchased to charge the EVs batteries is not used for en-route discharging phases but is provided back to the grid thanks to V2G technology.
- All energy transactions from/to the grid are shown in Fig. 9. From this figure, we can see that the energy sale takes place during energy peak load demand. The amount of energy transferred from the grid during the non-operating time is comparable with the amount of energy transferred to the grid during the operating time. This is useful for energy providers for frequency regulation and energy balance issues for reducing operational costs.
- Furthermore, from Fig. 9, we can see that in the L2 scenarios almost all EVs are either in the energy sale phase or in the energy purchase phase. However, for L3 scenarios, EV battery charge/discharge pattern is different. It turns out that frequently during the day, in the same time interval, a part of EVs sells energy and a part buys it with reduced net energy transferred. L2 charge speed type could provide a comparable amount of electric energy to the grid than the fast charge L3 by using EVs equipped with batteries Q1 or Q2. This could incentivize installing electric columns type L2 instead of type L3 with high savings in terms of fixed investment costs. This observation is confirmed by the numerical application of Zhang et al. (2020). However, according to Yoon et al. (2019), adopting charging columns type L2 instead of type L3 could increase the EV fleet size and, consequently, increase fixed investment costs.

From Table 9, we can make remarks from a fleet management point of view:

- In all analyzed scenarios, the start-of-day EVs distribution among stations follows almost the same configuration. Therefore, it seems that it does not strongly depend on EVs battery energy capacity and on charging columns type speed. This result is obtained because the customers' demand is the same for all the scenarios and therefore the cars are positioned to satisfy the users.
- Comparing the start-of-day V2G EVs distribution of the V2G-CSS scenarios with the corresponding baseline ones, we can observe that this distribution is not greatly influenced by the V2G charge/discharge operations. This could depend on the relative weight of the two objective function terms already discussed above. Since the vehicles are positioned at the start-of-day mainly to meet customers'

Table 7b
Main V2G-CSS scenarios results.

V2G-CSS scenario	Obj. fun. value [€/day]	Obj. fun. Upper Bound [€/day]	Rel. gap [%]	V2G-CSS revenues KPI [€/day]	V2G profits KPI [€/day]	Energy sale revenues [€/day]	Energy purchase costs [€/day]	Average EVs usage [%]
L2Q1	1546.94	1570.59	1.53	1530.0	16.94	117.83	100.89	12.58
L2Q2	1575.98	1585.26	0.57	1550.0	25.98	152.46	126.48	12.83
L2Q3	1455.10	1585.15	8.94	1432.5	22.60	147.93	125.33	11.92
L3Q1	1466.91	1595.48	8.76	1435.0	31.91	267.66	235.75	11.96
L3Q2	1477.89	1617.55	9.68	1422.5	55.39	313.23	257.84	12.06
L3Q3	1600.90	1647.83	2.89	1537.5	63.41	442.13	378.73	12.94

Table 8
Energy transferred from/to the grid in the different proposed model scenarios.

Scenario	Energy transferred to the grid (V2G) - energy sold [kWh]			Energy transferred from the grid (G2V) - energy purchased [kWh]			Net energy transferred (V2G - G2V) [kWh]		
	Oper. time	Non-oper. time	Total	Oper. time	Non-oper. time	Total	Oper. time	Non-oper. time	Total
L2Q1	1804.2	120.2	1924.4	859.6	1268.7	2128.3	944.6	−1148.5	−203.9
L2Q2	2443.4	44.7	2488.1	810.2	1892.2	2702.4	1633.2	−1847.5	−214.3
L2Q3	2379.5	42.8	2422.3	887.5	1779.3	2666.8	1492.0	−1736.5	−244.5
L3Q1	3510.0	1085.4	4595.5	2605.5	2089.8	4695.3	904.5	−1004.4	−99.9
L3Q2	4264.0	990.6	5254.6	2683.4	2608.6	5292.0	1580.6	−1618.0	−37.4
L3Q3	6223.8	1364.4	7588.2	3908.9	3689.9	7598.8	2314.9	−2325.5	−10.6

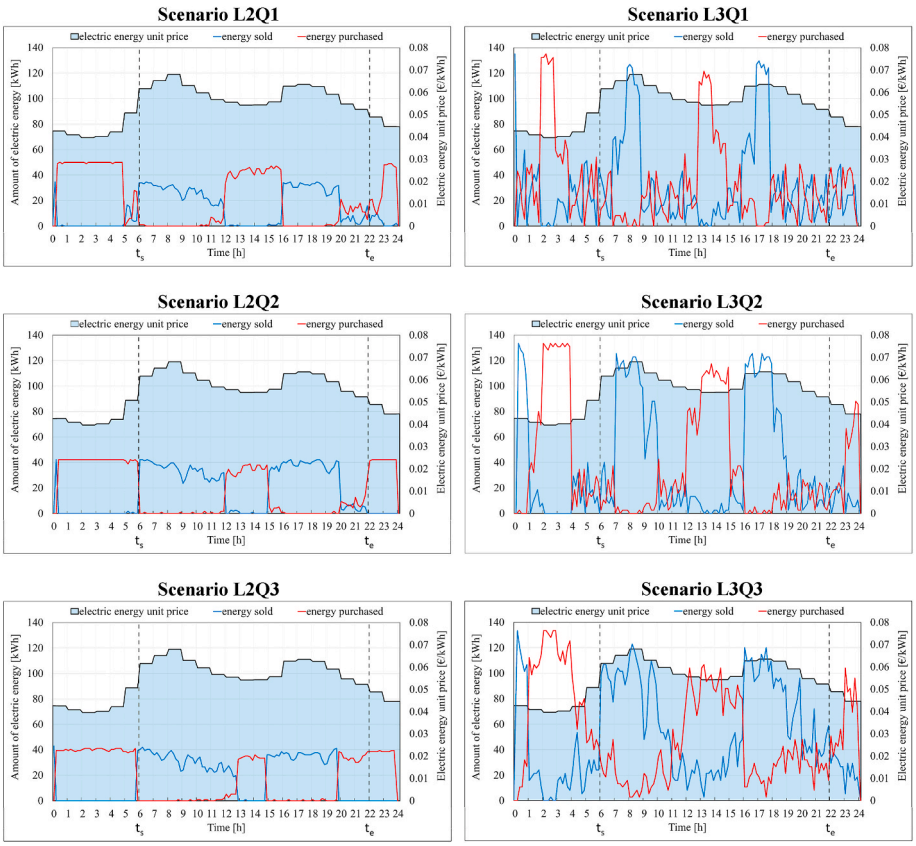

Fig. 9. Daily electric energy transactions for all V2G-CSS scenarios.

Table 9
Optimal EV distribution among stations i at the beginning of the day (time step $t = 1$) for the different scenarios.

Scenario	Station i																		
	1	2	3	4	5	6	7	8	9	10	11	12	13	14	15	16	17	18	19
B_L2Q1	0	0	0	0	0	2	0	0	0	3	9	2	6	0	2	6	1	9	10
L2Q1	0	0	0	0	0	2	0	0	0	2	10	3	6	0	2	6	1	8	10
B_L2Q2	0	0	0	0	0	1	0	0	0	3	9	3	6	0	1	7	1	9	10
L2Q2	0	0	0	0	0	2	0	0	0	1	9	4	7	0	2	7	0	8	10
B_L2Q3	0	0	0	0	0	1	0	0	0	3	7	2	8	0	1	8	1	9	10
L2Q3	0	0	0	0	0	4	0	0	0	2	7	4	7	0	2	5	1	8	10
B_L3Q1	0	0	0	0	0	1	0	0	0	2	7	3	9	0	1	7	1	9	10
L3Q1	0	0	0	0	0	2	0	0	0	3	6	3	5	0	3	7	3	8	10
B_L3Q2	0	0	0	0	0	2	0	0	0	1	8	4	8	0	2	6	0	9	10
L3Q2	0	0	1	0	0	4	0	0	0	5	8	2	4	1	1	6	0	8	10
B_L3Q3	0	0	0	0	0	1	0	0	0	2	9	4	6	0	1	6	2	9	10
L3Q3	0	0	0	0	0	0	0	0	0	3	10	2	7	0	2	7	0	9	10

demand, and the SOC of each vehicle at the end of the day are similar to that of the start-of-day (see Fig. 10), the relocation costs of the V2G-CSS scenarios could be comparable to those of the baseline ones.

From Fig. 10, we can make the following considerations:

- EV batteries charging occurs mainly in three times of the day when the price of energy is relatively low compared to the other periods, i.e., between 0:00 a.m. and 6:00 a.m., between 12:00 p.m. and 4:00 p.m. and between 8:00 p.m. and 0:00 a.m.
- The charge and V2G discharge slopes are greater the faster the charge and the lower the batteries capacity. In other words, these slopes are the lowest in the L2Q3 scenario and the highest in the L3Q1 scenario and grow according to the following order: L2Q3, L2Q2, L2Q1, L3Q3, L3Q2, L3Q1. For this reason, the L2Q3 scenario turns out to be the least constrained, i.e., the EVs start-of-day SOC is neither low nor the same for all vehicles. As the charge/discharge slopes increase (e.g., L2Q1 scenario), all vehicles assume almost the same and lower start-of-day SOC to maximize the objective function. For all vehicles, the SOC at the end of the day is very similar to the one at the beginning of the day and this can approximately guarantee the SOC continuity between one day and the next, representing the average operations of the system.
- For scenarios with higher charging speeds, SOCs fluctuate around the maximum or minimum values for a more extended period. During these periods, the energy prices are increasing, and therefore, the fluctuations are due to successive phases of energy purchase and sale.

5. Conclusions and further developments

Vehicle-to-Grid (V2G) technology allows electric energy transfer

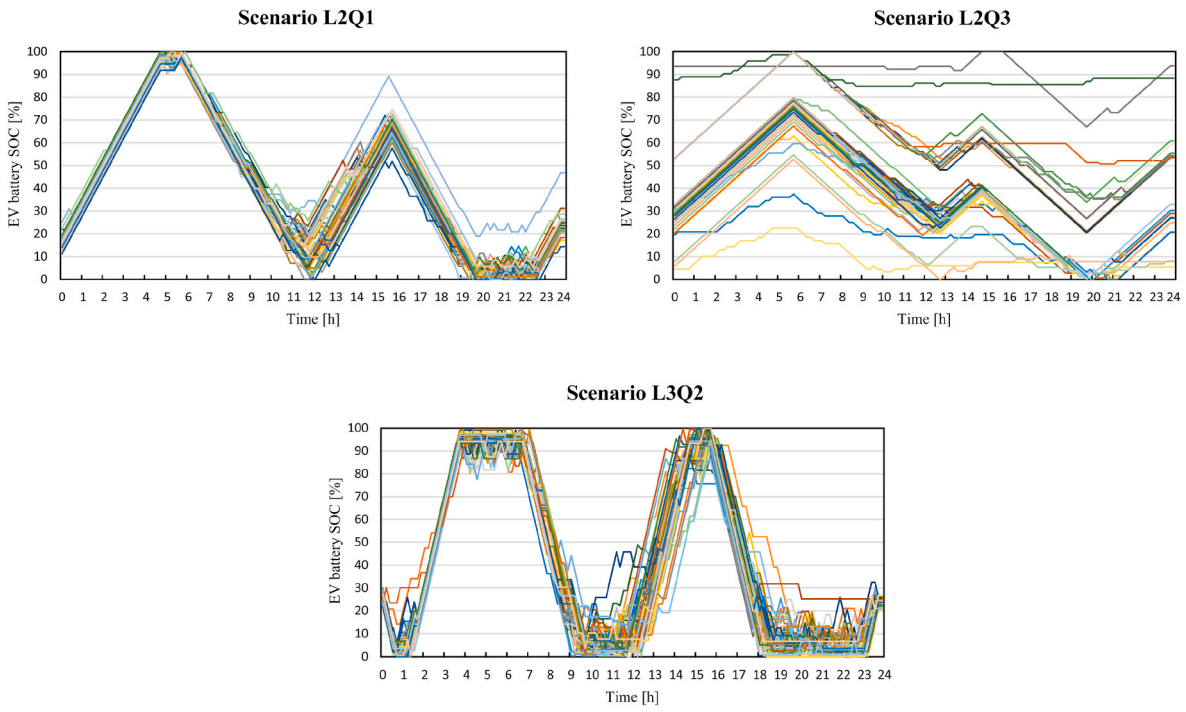

Fig. 10. Daily EV battery SOC for main V2G-CSS scenarios.

from vehicles to the grid. It can create benefits both for electric vehicles (EVs) owners and for grid operators/societies. For the former, V2G can be a source of income by selling previously purchased energy at a higher price. For the latter, it can be used, for example, for peak loading/frequency regulation adopting EV batteries as a source of energy storage. V2G technology is already on the market with some electric car models and bi-directional charging columns, but the V2G applications are currently mainly reserved for pilot projects. Given the growing electric car demand and the regulations that different countries are recently adopting, V2G could spread on a large scale and could be implemented for private users and private/public EVs fleet companies.

Although V2G applications to a Car-Sharing System (V2G-CSS) have not yet been realized on a large scale, in the literature, some authors have started to evaluate the profitability of this technology when associated with CSSs. In this work, we have proposed a novel Mixed Integer Linear Programming formulation that determines EVs distribution among stations at the beginning of the day and suggests the optimal daily EVs charging/discharging schedules. In particular, the objective of the problem is to maximize the sum of revenues from system users and V2G profits. The proposed model can manage both linear and non-linear EV charging/discharging energy rates by assuming a constant (M_C model) and a piecewise linear (M_PL model) EV charging/discharging function, respectively. V2G-CSS revenues and V2G profits are obtained according to mean expected daily customers demand and energy sale/purchase criterion based on mean expected day-ahead market electric energy price variation. This model can be applied to evaluate the possible average daily profitability of V2G operations starting from a fixed fleet and V2G-CSS size. We tested the effectiveness of proposed model on a small and a large-size test network assuming mean V2G-CSS demand and energy prices as known. However, for the real case network, only the proposed model with constant EV charging/discharging energy rates (M_C model) can be effectively used to find results in a reasonable computation time. Additionally, we carried out a sensitivity analysis by varying battery charge/discharge speed and capacities and compared the results with CSS baseline scenarios without considering the bidirectionality of the charge. Results have shown V2G profitability and a contribution to the grid during energy peak load demand in terms of energy-share without significantly reducing the satisfied V2G-CSS demand compared to the baseline cases.

Under the model assumptions, in each sensitivity analysis scenario, V2G profits are positive and on average equal to 36.04 €/day for a fleet of 50 EVs. Therefore, the adoption of V2G technology allows to fully cover the daily charging costs due to users' trips and obtain V2G profits by taking advantage of EVs unused time. Indeed, for the large-size network, EVs are used by customers for only about 12% of the operating day. For the rest of the time, without bi-directional charging, they would be parked not generating revenues for CSS companies. Most of the energy purchased to charge the EVs batteries is provided back to the grid during energy peak load demand, creating benefits also for energy providers. The net energy transferred to the grid during the operating time resulted to be significant, especially for lower charge speed type. These positive results were found under less-than-ideal V2G-CSS demand level and energy price conditions. The considered expected demand completely saturates the V2G-CSS. Therefore, the EVs are parked and enabled to transfer energy for shorter periods than in lower demand cases. Moreover, much of the V2G profits depend on energy prices fluctuations. The greater the differences in prices during the day, the greater the profits could be. We assumed average day-ahead electric energy prices. This means that greater differences between minimum and maximum prices can occur in some days, and consequently, higher V2G profits could be obtained.

The optimal start-of-day EVs distribution among the stations is different but very similar for each analyzed scenario (including the baseline ones without V2G) given the prevalence of V2G-CSS revenues over V2G profits. Therefore, it appears that the EVs are positioned at the beginning of the day mainly to meet expected customers' demand.

The optimal daily EVs charging/discharging schedules generally show three charging phases carried out when the price of energy is relatively low and two discharging phases performed during the rest of the day. The schedules turn out to be much smoother (without fluctuations) for low charging/discharging speeds and low battery capacities scenarios. From the battery degradation point of view, low charging/discharging speeds may be preferable, especially without adequate temperature management (Wu et al., 2019; Feng et al., 2020). However,

in the proposed model, the optimal charge/discharge schedules search does not consider possible battery degradation. Indeed, EV battery degradation depends on several factors (such as temperature, depth of discharge, C-rate) and not only on the parameters used in our work (battery SOC charging/discharging interval). There are conflicting opinions regarding the greater loss of capacity over time of the batteries used for V2G in literature. Uddin et al. (2017) show that through a smart grid algorithm with depth of discharge and overall cycling control, V2G technology can actually reduce battery degradation.

The integration of a detailed/empirical battery model with the proposed optimization is beyond the scope of this work. The proposition of a smart grid algorithm for managing battery lifetime in a car-sharing system with V2G technology will be presented in a future study. In this model, different aspects related to battery degradation can be considered assuming a non-linear battery charge/discharge pattern and optimized depth of discharge, charging/discharging speed, and minimum/maximum SOC levels. Future developments may also concern profit maximization models based on uncertain CSS demand and dynamic charging/discharging schedules. The proposed model is based on mean demand data and energy prices and is suitable for preliminary assessment on V2G profitability. Therefore, for large-scale networks with day by day and/or real-time car-sharing system and V2G management, implementing a heuristic algorithm to improve computation time would also be interesting. A further challenge might be the integration of the proposed model with the CSS network design for optimizing the position and the number of stations, as well as the number of parking places, EVs, and V2G charging/discharging columns considering different time horizons, customer demand, and electricity markets. Following this model, it could be interesting to evaluate a detailed cost-benefit analysis and calculate the effective V2G profitability applied to a real case study. Furthermore, different incentive policies may play a crucial role in promoting car-sharing mobility systems and, therefore, moving towards a large-scale V2G implementation.

In addition, the proposed model may not only be limited to the CSSs application but also, as a future study, for evaluating the V2G energy and economic profitability by coupling EVs with renewable energy sources and/or smart buildings (e.g., residential or office buildings) in a smart grid framework.

CRediT authorship contribution statement

Luigi Pio Prencipe: Conceptualization, Methodology, Software, Formal analysis, Writing – original draft, Writing – review & editing, Visualization. **J. Theresia van Essen:** Methodology, Formal analysis, Supervision, Writing – review & editing. **Leonardo Caggiani:** Conceptualization, Writing – original draft, Writing – review & editing. **Michele Ottomanelli:** Supervision, Writing – review & editing. **Gonçalo Homem de Almeida Correia:** Writing – review & editing.

Declaration of competing interest

The authors declare that they have no known competing financial interests or personal relationships that could have appeared to influence the work reported in this paper.

Data availability

No data was used for the research described in the article.

Acknowledgments

The authors are grateful to Dr. Xiao Liang for the research support and data provided on the Delft network. Special thanks go to Delft University of Technology for three months of visiting research period at the Delft Institute of Applied Mathematics. We also thank Dr. Giovanni Caramia for his support and availability to use the Department of Mechanics, Mathematics and Management of Polytechnic University of Bari laboratory computers.

References

Alfian, G., Rhee, J., Yoon, B., 2014. A simulation tool for prioritizing product-service system (PSS) models in a carsharing service. Comput. Ind. Eng. 70, 59–73.
Arfeen, Z.A., Khairuddin, A.B., Larik, R.M., Saeed, M.S., 2019. Control of distributed generation systems for microgrid applications: A technological review. Int. Trans. Electr. Energy Syst. 29 (9), e12072.
Axsen, J., Sovacool, B.K., 2019. The roles of users in electric, shared and automated mobility transitions. Transport. Res. Transport Environ. 71, 1–21.
Barth, M., Todd, M., 1999. Simulation model performance analysis of a multiple station shared vehicle system. Transport. Res. C Emerg. Technol. 7 (4), 237–259.
Barth, M., Todd, M., Xue, L., 2004. User-based Vehicle Relocation Techniques for Multiple-Station Shared-Use Vehicle Systems. Transportation Research Board 83rd Annual Meeting.
Bishop, J.D.K., Axon, C.J., Bonilla, D., Tran, M., Banister, D., McCulloch, M.D., 2013. Evaluating the impact of V2G services on the degradation of batteries in PHEV and EV. Appl. Energy 111, 206–218.
Boyacı, B., Zografos, K.G., Geroliminis, N., 2015. An optimization framework for the development of efficient one-way car-sharing systems. Eur. J. Oper. Res. 240, 718–733.
Brendel, A.B., Lichtenberg, S., Brauer, B., Nastjuk, I., Kolbe, L.M., 2018. Improving electric vehicle utilization in carsharing: a framework and simulation of an e-carsharing vehicle utilization management system. Transport. Res. Transport Environ. 64, 230–245.
Caggiani, L., Prencipe, L.P., Ottomanelli, M., 2020. A static relocation strategy for electric car-sharing systems in a vehicle-to-grid framework. Transport. Lett. 13 (3), 219–228.
Cai, H., Chen, Q., Guan, Z., Huang, J., 2018. Day-ahead optimal charging/discharging scheduling for electric vehicles in microgrids. Protect. Control Mod. Power Sys. 3, 9.
CHAdeMO Association, 2021. Technology overview. Retrieved. https://www.chademo.com/technology/technology-overview/. (Accessed 10 January 2021).
Ciari, F., Bock, B., Balmer, M., 2014. Modeling Station-Based and Free-Floating Carsharing Demand: Test Case Study for Berlin. Transport. Res. Rec. 2416 (1), 37–47.
Contreras, J., Espinola, R., Nogales, F.J., Conejo, A.J., 2003. ARIMA models to predict next-day electricity prices. IEEE Trans. Power Syst. 18 (3), 1014–1020.
Correia, G.H.A., Antunes, A.P., 2012. Optimization approach to depot location and trip selection in one-way carsharing systems. Transport. Res. Part E 48, 233–247.
Correia, G.H.A., van Arem, B., 2016. Solving the user optimum privately owned automated vehicles assignment problem (UO-POAVAP): a model to explore the impacts of self-driving vehicles on urban mobility. Transport. Res. Part B 87, 64–88.
Correia, G.H.A., Jorge, D.R., Antunes, D.M., 2014. The added value of accounting for users flexibility and information on the potential of a station-based one-way car-sharing system: an application in Lisbon, Portugal. J. Intell. Transport. Syst. Technol. Plann. Oper. 18, 299–308.
Dallinger, D., Krampe, D., Wietschel, M., 2011. Vehicle-to-grid regulation reserves based on a dynamic simulation of mobility behavior. IEEE Trans. Smart Grid 2 (2), 302–313.
de Almeida, A., Fonseca, P., Schlomann, B., Feilberg, N., 2011. Characterization of the household electricity consumption in the EU, potential energy savings and specific policy recommendations. Energy Build. 43 (8), 1884–1894.
De Brey, B., 2017. Smart solar charging: Bi-directional AC charging (V2G) in The Netherlands. J. Energy Power Eng. 11, 483–490.
Di Febbraro, A., Sacco, N., Saeednia, M., 2012. One-way carsharing: solving the relocation problem. Transport. Res. Rec. 2319, 113–120.
Dubarry, M., Devie, A., McKenzie, K., 2017. Durability and reliability of electric vehicle batteries under electric utility grid operations: bidirectional charging impact analysis. J. Power Sources 358, 39–49.
Enel. Retrieved July 10, 2020, from https://corporate.enel.it/en/stories/a/2017/05/V2G-the-car-of-the-future-is-a-battery.
Engie-FCA project. Retrieved July 15, 2020, from https://engie-eps.com/corporate/work-has-begun-at-mirafiori-on-the-fca-engie-eps-vehicle-to-grid-pilot-project.
Fan, Z., 2012. A distributed demand response algorithm and its application to PHEV charging in smart grids. IEEE Trans. Smart Grid 3 (3), 1280–1290.
Fastned, 2021. Retrieved December 15, 2021, from https://v2g.co.uk/2018/07/fastned-electric-vehicle-charging-profiles.
Feng, J., Hou, S., Yu, L., Dimov, N., Zheng, P., Wang, C., 2020. Optimization of photovoltaic battery swapping station based on weather/traffic forecasts and speed variable charging. Appl. Energy 264, 114708.
Fink, A., Reiners, T., 2006. Modeling and solving the short-term car rental logistics problem. Transport. Res. E Logist. Transport. Rev. 42, 272–292.
Firnkorn, J., Müller, M., 2011. What will be the environmental effects of new free-floating car-sharing systems? the case of car2go in ulm. Ecol. Econ. 70 (8), 1519–1528.
Fournier, G., Lindenlauf, F., Baumann, M., Seign, R., Weil, M., 2014. Carsharing with electric vehicles and vehicle-to-grid: a future business model?. In: Radikale Innovationen in der Mobilität Technische und betriebswirtschaftliche Aspekte, pp. 63–79.
Freund, D., Raab, A.F., Küster, T., Albayrak, S., Strunz, K., 2012. Agent-based Integration of an Electric Car Sharing Fleet into a Smart Distribution Feeder. 3rd IEEE PES, Berlin, Germany, pp. 1–8.

Fu, F., Dong, H., 2019. Targeted optimal path problem for electric vehicles with connected charging stations. PLoS One 14 (8), e0220361.
Gambella, C., Malaguti, E., Masini, F., Vigo, D., 2018. Optimizing relocation operations in electric car-sharing. Omega 81, 234–245.
Guille, C., Gross, G., 2009. A conceptual framework for the vehicle-to-grid (V2G) implementation. Energy Pol. 37, 4379–4390.
Han, S., Han, S., Sezaki, K., 2010. Development of an optimal vehicle-to-grid aggregator for frequency regulation. IEEE Trans. Smart Grid 1 (1), 65–72.
Heilmann, C., Friedl, G., 2021. Factors influencing the economic success of grid-to-vehicle and vehicle-to-grid applications-A review and meta-analysis. Renew. Sustain. Energy Rev. 145, 111115.
Herrmann, S., Schulte, F., Voß, S., 2014. Increasing acceptance of free-floating car sharing systems using smart relocation strategies: a survey based study of car2go Hamburg. Int. Conf. Comput. Logist. 151–162.
Hiermann, G., Puchinger, J., Ropke, S., Hartl, R.F., 2016. The electric fleet size and mix vehicle routing problem with time windows and recharging stations. Eur. J. Oper. Res. 252 (3), 995–1018.
Hof, J., Schneider, M., Goeke, D., 2017. Solving the battery swap station location-routing problem with capacitated electric vehicles using an AVNS algorithm for vehicle-routing problems with intermediate stops. Transp. Res. Part B Methodol. 97, 102–112.
Iacobucci, R., McLellan, B., Tezuka, T., 2019. Optimization of shared autonomous electric vehicles operations with charge scheduling and vehicle-to-grid. Transport. Res. C Emerg. Technol. 100, 34–52.
IEA, 2020. Global EV Outlook 2020. Retrieved. https://www.iea.org/reports/global-ev-outlook-2020. (Accessed 6 July 2020).
IEA, 2021. Global EV Outlook 2021. Retrieved. https://www.iea.org/reports/global-ev-outlook-2021. (Accessed 6 January 2021).
Illgen, S., Höck, M., 2018. Electric vehicles in car sharing networks – challenges and simulation model analysis. Transport. Res. Transport Environ. 63, 377–387.
Illgen, S., Höck, M., 2019. Literature review of the vehicle relocation problem in one-way car sharing networks. Transp. Res. Part B Methodol. 120, 193–204.
Jamshidi, H., Correia, G.H.A., van Essen, J.T., Nökel, K., 2021. Dynamic planning for simultaneous recharging and relocation of shared electric taxies: a sequential MILP approach. Transport. Res. C Emerg. Technol. 125, 102933.
Jiang, L., Hu, G., 2018. A Review on Short-Term Electricity Price Forecasting Techniques for Energy Markets, 15th International Conference on Control, Automation, Robotics and Vision (ICARCV), Singapore, Japan, pp. 937–944.
Jorge, D., Correia, G.H.A., Barnhart, C., 2014. Comparing optimal relocation operations with simulated relocation policies in one-way carsharing systems. IEEE Trans. Intell. Transport. Syst. 15, 1667–1775.
Jorge, D., Barnhart, C., Correia, G.H.A., 2015a. Assessing the viability of enabling a round-trip carsharing system to accept one-way trips: application to Logan Airport in Boston. Transport. Res. C Emerg. Technol. 56, 359–372.
Jorge, D., Molnar, G., Correia, G.H.A., 2015b. Trip pricing of one-way station-based carsharing networks with zone and time of day price variations. Transp. Res. Part B Methodol. 81 (2), 461–482.
Jung, J., Koo, Y., 2018. Analyzing the effects of car sharing services on the reduction of greenhouse gas (GHG) emissions. Sustainability 10, 539.
Kaur, K., Kumar, N., Singh, M., 2019. Coordinated power control of electric vehicles for grid frequency support: MILP-based hierarchical control design. IEEE Trans. Smart Grid 10 (3), 3364–3373.
Kek, A.G.H., Cheu, R.L., 2006. Relocation simulation model for multiple-station shared-use vehicle systems. J. Transport. Res. Board 1, 81–88.
Kek, A.G.H., Cheu, R.L., Meng, Q., Fung, C.H., 2009. A decision support system for vehicle relocation operations in carsharing systems. Transport. Res. E Logist. Transport. Rev. 45 (1), 149–158.
Kempton, W., Kubo, T., 2000. Electric-drive vehicles for peak power in Japan. Energy Pol. 28 (1), 9–18.
Kempton, W., Letendre, S.E., 1997. Electric vehicles as a new power source for electric utilities. Transport. Res. Transport Environ. 2, 157–175.
Kempton, W., Tomic, J., 2005a. Vehicle-to-grid power fundamentals: calculating capacity and net revenue. J. Power Sources 144 (1), 268–279.
Kempton, W., Tomic, J., 2005b. Vehicle-to-grid power implementation: from stabilizing the grid to supporting large-scale renewable energy. J. Power Sources 144 (1), 280–294.
Kempton, W., Tomic, J., Letendre, S., Brooks, A., Lipman, T., 2005. Vehicle-to-grid Power: Battery, Hybrid and Fuel Cell Vehicles as Resources for Distributed Electric Power in California. Institute of Transportation Studies, Davis, CA.
Khalen, M.T., Ketter, W., van Dalen, J., 2018. Electric vehicle virtual power plant dilemma: grid balancing versus customer mobility. Prod. Oper. Manag. 27, 2054–2070.
Kolawole, O., Al-Anbagi, I., 2019. Electric vehicles battery wear cost optimization for frequency regulation support. IEEE Access 7, 130388–130398.
Kongjeen, Y., Bhumkittipich, K., 2018. Impact of plug-in electric vehicles integrated into power distribution system based on voltage-dependent power flow analysis. Energies 11, 1571.
Krause, E.F., 1973. Taxicab geometry. Math. Teach. 66, 695–706.
Lassila, J., Haakana, J., Tikka, V., Partanen, J., 2012. Methodology to analyze the economic effects of electric cars as energy storages. IEEE Trans. Smart Grid 3 (1), 506–516.
Nissan Leaf, 2019. Retrieved August 4, 2020, from https://www.nissanusa.com/content/dam/Nissan/us/vehicle-brochures/2019/2019-nissan-nissan-leaf-brochure-en.pdf.
Li, Q., Liao, F., Timmermans, H.J., Huang, H., Zhou, J., 2018. Incorporating free-floating car-sharing into an activity-based dynamic user equilibrium model: a demand-side model. Transp. Res. Part B Methodol. 107, 102–123.
Li, Z., Su, S., Jin, X., Chen, H., 2021a. Distributed energy management for active distribution network considering aggregated office buildings. Renew. Energy 180, 1073–1087.
Li, Z., Su, S., Jin, X., Chen, H., Li, Y., Zhang, R., 2021b. A hierarchical scheduling method of active distribution network considering flexible loads in office buildings. Int. J. Electr. Power Energy Syst. 131, 106768.
Li, Q., Zhao, D., Li, X., Wang, X., 2022. Electric vehicle sharing based "energy sponge" service interfacing transportation and power systems. Clean. Logist. Supply Chain 3, 100022.
Liang, X., Correia, G.H.A., van Arem, B., 2018. Applying a Model for Trip Assignment and Dynamic Routing of Automated Taxis with Congestion: System Performance in the City of Delft, The Netherlands. Transportation Research Record Journal of the Transportation Research Board, pp. 1–11.
Liang, X., Correia, G.H.A., An, K., van Arem, B., 2020. Automated taxis' dial-a-ride problem with ride-sharing considering congestion-based dynamic travel times. Transport. Res. C Emerg. Technol. 112, 260–281.
Liu, H., Zhang, Y., Ge, S., Gu, C., Li, F., 2019. Day-ahead scheduling for an electric vehicle PV-based battery swapping station considering the dual uncertainties. IEEE Access 7, 115625–115636.
Lunz, B., Yan, Z., Gerschler, J.B., Sauer, D.U., 2012. Influence of plug-in hybrid electric vehicle charging strategies on charging and battery degradation costs. Energy Pol. 46, 511–519.
Machado, C.A.S., Hue, N.P.M.de, Berssaneti, F.T., Quintanilha, J.A., 2018. An overview of shared mobility. Sustainability 10, 4342.
Mamalis, T., Bose, S., Varshney, L.R., 2019. Business-to-Peer carsharing systems with electric vehicles. 53rd Ann. Conf. Inform. Sci. Sys. 1–6.
Martin, E., Shaheen, S., 2011. The impact of carsharing on public transit and non-motorized travel: an exploration of North American carsharing survey data. Energies 4, 2094–2114.
Meelen, T., Doody, B., Schwanen, T., 2021. Vehicle-to-Grid in the UK fleet market: an analysis of upscaling potential in a changing environment. J. Clear. Product. 290, 125203.
Modumudi, V.G., 2019. Master Thesis. Review of Vehicle-To-Grid Implementation in Pilot Program.
Montoya, A., Guéret, C., Mendoza, J.E., Villegas, J.G., 2017. The electric vehicle routing problem with nonlinear charging function. Transp. Res. Part B Methodol. 103, 87–110.
Nair, R., Miller-Hooks, E., 2010. Fleet management for vehicle sharing operations. Transport. Sci. 45, 524–540.
Nair, R., Miller-Hooks, E., 2014. Equilibrium network design of shared-vehicle systems. Eur. J. Oper. Res. 235, 47–61.
Noel, L., Zarazua de Rubens, G., Kester, J., Sovacool, B.K., 2019. Vehicle-to-Grid: A Sociotechnical Transition beyond Electric Mobility. Palgrave Macmillan, Cham.
Noel, L., de Rubens, G.Z., Kester, J., Sovacool, B.K., 2021. Leveraging user-based innovation in vehicle-to-X and vehicle-to-grid adoption: a Nordic case study. J. Clear. Product. 287, 125591.
Nourinejad, M., Roorda, M., 2015. Carsharing operations policies: a comparison between one-way and two-way systems. Transportation 42 (3), 497–518.
Nuvve, 2020. Projects. https://nuvve.com/projects/. (Accessed 4 August 2020).
Pavic, I., Capuder, T., Kuzle, I., 2015. Value of flexible electric vehicles in providing spinning reserve services. Appl. Energy 157, 60–74.
Pelletier, S., Jabali, O., Laporte, G., Veneroni, M., 2017. Battery degradation and behaviour for electric vehicles: review and numerical analyses of several models. Transport. Res. Part B 103, 158–187.
Prinz, C., Willnat, M., Brendel, A.B., Lichtenberg, S., Kolbe, L.M., 2021. CASSI: design of a simulation environment for vehicle relocation in carsharing. AIS Trans. Hum.-Comput. Interact. 13 (1), 12–37.
Ravi, S.S., Aziz, M., 2022. Utilization of electric vehicles for vehicle-to-grid services: progress and perspectives. Energies 15, 589.
Requia, W.J., Mohamed, M., Higgins, C.D., Arain, A., Ferguson, M., 2018. How clean are electric vehicles? Evidence-based review of the effects of electric mobility on air pollutants, greenhouse gas emissions and human health. Atmos. Environ. 185, 64–77.
Rezvanizaniani, S.M., Liu, Z., Chen, Y., Lee, J., 2014. Review and recent advances in battery health monitoring and prognostics technologies for electric vehicle (EV) safety and mobility. J. Power Sources 256, 110–124.
Rogers, K.M., Klump, R., Khurana, H., Aquino-Lugo, A.A., Overbye, T.J., 2010. An authenticated control framework for distributed voltage support on the smart grid. IEEE Trans. Smart Grid 1 (1), 40–47.
Rotering, N., Ilic, M., 2011. Optimal charge control of plug-in hybrid electric vehicles in deregulated electricity markets. IEEE Trans. Power Syst. 26 (3), 1021–1029.
Saber, A.Y., Venayagamoorthy, G.K., 2010. Intelligent unit commitment with vehicle-to-grid —a cost-emission optimization. J. Power Sources 195 (3), 898–911.
Santos, G.G.D., Correia, G.H.A., 2019. Finding the relevance of staff-based vehicle relocations in one-way carsharing systems through the use of a simulation-based optimization tool. J. Intell. Transport. Sys. 1–22.
Shuman, L., Yang, W., 2019. A two-stage supervised learning approach for electricity price forecasting by leveraging different data sources. Appl. Energy 242, 1497–1512.
Shuyun, R., Fengji, L., Lei, L., Shu-Chien, H., Xuran, I.L., 2019. A novel dynamic pricing scheme for a large-scale electric vehicle sharing network considering vehicle relocation and vehicle-grid-integration. Int. J. Prod. Econ. 218, 339–351.
SMARD, 2019. Retrieved January 10, 2019, from https://www.smard.de/en.
Sovacool, B.K., Noel, L., Axsen, J., Kempton, W., 2018. The neglected social dimensions to a vehicle-to-grid (V2G) transition: a critical and systematic review. Environ. Res. Lett. 13, 013001.

Sprei, F., Habibi, S., Englund, C., Pettersson, S., Voronov, A., Wedlin, J., 2019. Free-floating car-sharing electrification and mode displacement: travel time and usage patterns from 12 cities in Europe and the United States. Transport. Res. Transport Environ. 71, 127–140.
Taiebat, M., Xu, M., 2019. Synergies of four emerging technologies for accelerated adoption of electric vehicles: shared mobility, wireless charging, vehicle-to-grid, and vehicle automation. J. Clean. Prod. 230, 794–797.
Thompson, A.W., 2018. Economic implications of lithium ion battery degradation for Vehicle-to-Grid (V2X) services. J. Power Sources 396, 691–709.
Tomic, J., Kempton, W., 2007. Using fleets of electric-drivers vehicles for grid support. J. Power Sources 168 (2), 459–468.
Uddin, K., Jackson, T., Widanage, W.D., Chouchelamane, G., Jennings, P.A., Marco, J., 2017. On the possibility of extending the lifetime of lithium-ion batteries through optimal V2G facilitated by an integrated vehicle and smart-grid system. Energy 133, 710–722.
Uddin, K., Dubarry, M., Glick, M.B., 2018. The viability of vehicle-to-grid operations from a battery technology and policy perspective. Energy Pol. 113, 342–347.
Ul-Haq, A., Cecati, C., Al-Ammar, E., 2016. Modeling of a photovoltaic-powered electric vehicle charging station with vehicle-to-grid implementation. Energies 10, 4.
WeDriveSolar, 2020. Retrieved July 10, 2020, from https://www.v2g-hub.com/projects/utrecht-v2g-charge-hubs-we-drive-solar.
Williams, B.D., Kurani, K.S., 2006. Commercializing light-duty plug-in/plug-out hydrogen-fuel-cell vehicles: "Mobile Electricity" technologies and opportunities. J. Power Sources 166 (7), 549–566.
Wu, W., Wang, S., Wu, W., Chen, K., Hong, S., Lai, Y., 2019. A critical review of battery thermal performance and liquid based battery thermal management. Energy Convers. Manag. 182, 262–281.
Yilmaz, M., Krein, P.T., 2013. Review of the impact of vehicle-to-grid technologies on distribution systems and utility interfaces. IEEE Trans. Power Electron. 28 (12), 5673–5689.
Yoon, T., Cherry, C.R., Ryerson, M.S., Bell, J.E., 2019. Carsharing demand estimation and fleet simulation with EV adoption. J. Clean. Prod. 206, 1051–1058.
Zhang, P., Qian, K., Zhou, C., Stewart, B.G., Hepburn, D.M., 2012. A methodology for optimization of power systems demand due to electric vehicle charging load. IEEE Trans. Power Syst. 27 (3), 1628–1636.
Zhang, Yiling, Lu, Mengshi, Shen, Siqian, 2020. On the Values of Vehicle-to-Grid Electricity Selling in Electric Vehicle Sharing. Manuf. Serv. Oper. Manag. Man 23 (2), 488–507.